Non-destructive methods for predicting sawn lumber properties from young, standing *Eucalyptus grandis* and *Eucalyptus grandis X urophylla* trees.

by

Ashlee Cherice Prins

Thesis presented in partial fulfilment of the requirements for the degree of

Master of Science

at

Stellenbosch University

Department of Forest and Wood Sciences, Faculty of AgriSciences

Supervisor: Prof Brand Wessels

March 2021

Declaration

By submitting this thesis electronically, I declare that the entirety of the work contained therein is my own, original work, that I am the sole author thereof (save to the extent explicitly otherwise stated), that reproduction and publication thereof by Stellenbosch University will not infringe any third party rights and that I have not previously in its entirety or in part submitted it for obtaining any qualification.

Date: 5 March 2021

Abstract

Eucalyptus is the most widely planted hardwood genus in South Africa cultivated for both sawn lumber and pulp. It is known for its fast growth but is prone to high growth stresses and other problematic wood properties. The properties with the highest impact on *Eucalyptus* sawn lumber quality are excessive board splits, severe shrinkage, brittle heart and cell collapse. This study aims to identify and evaluate methods to non-destructively test the underlying properties in **standing** *Eucalyptus grandis* and *Eucalyptus grandis X urophylla* **trees** related to these lumber properties and to develop a predictive tool for identifying superior (plus) trees, for applications within tree breeding programmes. A secondary objective was assessing variation within and between trees for the measured properties.

70 trees, sampled from five sites close to Tzaneen, Limpopo, were split into six sample groups. Five of these groups consisted of 10 trees each, whilst the sixth group consisted of 20 trees due to the genetic variation of the trees on the site. The trees were chosen based on age and genetic improvement – two characteristics which were considered as important determinants for lumber quality. A novel paddle core system was developed for assessing growth strain within the stem of the standing tree. Additionally, non-invasive measurements of sound-wave velocity, height and diameter were taken before felling the tree. The felled trees were crosscut into two logs and four discs for further assessment. The logs were milled into boards and kiln dried for evaluating shrinkage, split length, brittle heart and collapse. The discs were processed for moisture content and density measurements.

Property analysis of the boards showed that both split length and brittle heart increased with age and decreased with radial position from the pith to bark, as well as decreased with height. Cell collapse proved to be centered around the pith, with significantly higher levels of collapse exhibited in the boards closer to the pith and little to no collapse in the boards closer to the periphery. Width and thickness shrinkage exhibited opposite trends where width shrinkage increased from pith to bark, while thickness shrinkage had a decreasing trend. Density presented a V-trend for all six groups with density decreasing just after the pith, and then increasing towards the bark. Strain measurements produced varying results between the two different tools used to mark the paddle cores. One tool indicated only compressive strain whilst the other indicated only tensile strain in the given stem. Moisture content increased with height. Time-of-Flight (ToF) of stress waves decreased with age and increased for trees that were

improved through genetic selection. Cup had various radial trends for different groups and bow increased from pith to bark.

Moisture content, density, time-of-flight and growth strain were used to develop models for predicting the occurrence of the aforementioned lumber properties. It was not possible to develop models that predicted lumber properties reliably over the six age and genotype groups. The best model for predicting split length of the boards showed promise on young trees with a marginal coefficient of determination (r^2) of 0.772. The input variables that can be measured on standing trees in this model were time-of-flight, moisture content and growth strain. Moisture content and strain was measured on samples obtained via limited destructive means (as measured with the paddle core method). The end split scoring system of the tree, which was used in the past to predict log quality, was also compared to the measured board splits by means of simple linear regression, but a relatively poor coefficient of determination was obtained ($r^2 = 0.216$). The newly developed paddle core method has shown potential as a predictor of growth strain. However, further improvement is still required before practical implementation can be considered.

Opsomming

Eucalyptus is die mees wydverspreide loofhout genus in Suid Afrika en word verwerk vir beide gesaagde hout en pulp. Dit staan bekend vir sy vinnige groei maar is vatbaar vir hoë interne spanning en ander problematieke houteienskappe. Van die eienskappe behels spleting in planke, hoë krimpingsvlakke, ’n bros kern en selineenstorting. Hierdie studie was gemik op die identifikasie, ontwikkeling en evaluasie van nie-vernietigende toetsmetodes op staande *Eucalyptus grandis* en *Eucalyptus* g*randis X urophylla* bome. Die doelwit is om superieure (plus) bome te indentifiseer vir aanwending in boomveredelingsprogramme. ‘n Sekondêre doel was die beskrywing van houteienskapvariasie in -en tussen bome.

Sewentig boom-monsters van vyf areas naby Tzaneen, Limpopo, was verdeel in verskillende groepe. Vyf van hierdie groepe het bestaan uit 10 bome elk terwyl die sesde groep bestaan het uit 20 bome. Die bome was gekies volgens ouderdom en genetiese verbetering aangesien beide faktore gewoonlik ’n belangrike rol speel in houtkwaliteit. n Nuwe metode (“paddle core method”) was ontwikkel vir die assessering van die groeispannings binne die stam van staande bome. Addisionele lesings van klankgolfspoed, boomhoogte -en diameter was geneem alvorens die bome geoes was. Die geoesde bome was opgesny in twee gedeeltes en vier skywe is verwyder vir die meting van houteienskappe. Die stompe was in n saagmeul gesny na planke en oondgedroog vir evaluering van inkrimping, spleting, broskern en selineenstorting. Die skywe was geprosesseer vir toetsing van voginhoud en houtdigteid.

Analise van die planke toon dat spleetlengtes en broskern vermeerder het met ouderdom en verminder het met radiale posisie (kern tot by die bas) en verminder het met boomhoogte. Selineenstorting het meestal voorgekom rondom die kern, met min of geen ineenstorting in die planke nader aan die baskant. Breedte -en dikte-inkrimping toon teenoorgestelde neigings, met breedte-inkrimping wat vermeerder het vanaf die kern na die bas terwyl die dikte-inkrimping verminder het vanaf die kern na die bas. Digtheid het ‘n V-neiging getoon vir al ses groepe met ‘n digtheidsafname net na die kern en dan ’n toename nader aan die bas. Spanningsmetings het verslillende uitslae getoon vir die twee verskillende meetapparate wat gebruik is. Een apparaat het slegs drukspannings gewys terwyl die ander slegs trekspannings gewys het. Voginhoud het vermeerder met toename in boomhoogte. Die vlugtyd van klankgolwe het afgeneem met ouderdom en toegeneem vir bome wat deur genetiese seleksie verbeter is.

Voginhoud, houtdigtheid, klankspoed en groeispanning is gebruik om modelle te ontwikkel om die voorkoms van bogenoemde houteienskappe te voorspel. Dit was nie moontlik om modelle te ontwikkel wat houteienskappe betroubaar deur al die ouderdoms- en genetiese groepe voorspel nie. Die beste model om die spleetlengte van die planke te voorspel, het belofte getoon vir jong bome met ‘n marginale bepalingskoëffisiënt (r^2) van 0.772. Die invoerveranderlikes in hierdie model was klankspoed, voginhoud, en groeispanning. Die blokentspletingsmetode wat huidiglik gebruik word om plankspleting te voorspel is ook vergelyk met die gemete plankspletings, maar ‘n relatiwe swak bepalingskoëffisiënt is verkry (r^2 = 0.216). Die nuut ontwikkelde “paddle core method” het potensiaal getoon as n voorspeller van groeispanning. Verdere verbeterings is egter nog nodig voordat dit vir praktiese implementering oorweeg kan word.

"I dedicate this thesis to my stepfather, the late Lewis James Rodger Rodkin for encouraging me to take this step in my academic career, and to my mother, Ann Jeanetta McBryne, for her continuous support throughout this process."

Acknowledgements

I wish to acknowledge the following individuals, teams, and institutions for their contributions towards this research:

- Prof. Brand Wessels for his guidance and supervision throughout this process.
- Dr. Zahra Naghizadeh Mahani for her assistance and input in compiling this research thesis.
- Dr Justin Erasmus for his expertise and assistance with the statistical analysis.
- Ms. Sonia Du Buisson, Mr. George Dowse, Dr. Steve Verryn and the teams at Northern Timbers and their nursery division for their assistance and the sample material for this project.
- The staff and students of the Forest and Wood Sciences Department at Stellenbosch University for all their support and advice.
- The Hans Merensky Foundation for sponsoring this project.
- To my family and friends for their unwavering support, encouragement, and assistance through this journey.
- To those, who I have failed to mention above, I thank you.

Table of Contents

List of Figures

List of Tables

List of Equations

List of Abbreviations

ANOVA	Analysis of Variances
CSIR	Council for Scientific and Industrial Research
CT Scanning	Computed Tomography Scanning
DBH	Diameter at breast height
Marginal R^2	A pseudo R^2 calculated for the fixed effects only, of a linear mixed effects model. It is not a true R^2 but can be used to assess the fit of a mixed effects model.
MI	Mature Improved
MU	Mature Unimproved
MFA	Microfibril angle
MOE	Modulus of elasticity
MOR	Modulus of rupture
OLD	Old compartment group of trees, 23 years of age
Plus Tree	A superior tree with regards to strength and desired wood properties
ST	Splitting Trial
r	Correlation coefficient
R squared / R^2	Coefficient of determination.
ToF	Time of flight in µs
YI	Young Improved
YU	Young Unimproved

1 Introduction

1.1 Background

Eucalyptus is the most widely planted hardwood genus in South Africa. 41.8% of South Africa's total plantation area, 521 2264ha, is cultivated with *Eucalyptus* trees for sawn lumber and pulp (Godsmark, 2017). *Eucalyptus* stands in South Africa have rotation ages of between six to ten years for pulp, poles, fuel wood and mining lumber regimes, and thirty years or less for sawn lumber regimes (Orwa 2009). However, *Eucalyptus*' high growth rate possibly also plays a role in producing certain defects in the lumber namely severe growth stresses, warp, splitting, high shrinkage coefficients and brittle heart, all resulting in value reduction of the sawn lumber. Studies showed that genetics, age, radial position and height affect the extent to which some of these defects are manifested in logs and sawn boards (Malan, 1995) and that there can be vast within-tree and within-stand variations.

Over the years, there has been a growing effort to decrease the defects and improve wood properties for *Eucalyptus* sawn lumber through tree breeding using wood quality selection criteria together with the usual tree health and growth measures (Malan, 1995). Hans Merensky, in collaboration with the CSIR, started research on tree splitting trials to determine factors which may assist in predicting the future mature wood value for sawn wood and veneer from young trees in South Africa (Verryn 2000). This could potentially lead to an increase in the value of the lumber obtained from *Eucalyptus* plantations, as well as the yield (Malan 1995).

1.2 Problem Statement

Many *Eucalyptus* species are known for having high levels of growth stress, inducing the onset of brittle heart in the centre of the stem as well as causing logs and lumber to develop large splits after harvesting (Vermaas 2000). Many *Eucalyptus* species are also prone to cell collapse and high shrinkage coefficients after drying (Bariska 1992; Verryn 2000).

Brittle heart and cell collapse reduce the strength properties of the lumber by weakening its structural integrity (Desch 1981). Anisotropic shrinkage is one of the main reasons for warp during drying. Warped lumber requires additional machining such as planing to remove the defect, which subsequently leads to lower volume and value recovery. Similarly, with splitting,

volume recovery is also reduced as boards are required to be cut to smaller specifications to remove the split section.

In each of these examples, value is lost. Therefore, if the parameters affecting these properties can be determined and the extent of these defects can be assessed **before harvesting, or early in the rotation** (i.e. in the standing tree), superior properties can be identified and used for the intended purpose to breed future stands of higher value.

1.3 Research Objectives

Given the nature of *Eucalyptus grandis* and *Eucalyptus grandis X urophylla* species to develop the aforementioned defects, this research was aimed at finding methods of either limited or no destruction to identify the underlying properties related to these defects in trees (i.e. to obtain the needed data or samples without felling the tree or compromising its ability for continued growth). This research will also assess the suitability of using non-destructive methods as a predictive tool for identifying plus trees, for applications within tree breeding programmes to improve the overall lumber quality, harvested from future *Eucalyptus* stands.

The main objective of this project was thus to develop predictive models of **lumber** splitting, brittle heart, cell collapse and shrinkage in sawn boards of *Eucalyptus grandis* and *Eucalyptus grandis X uraphylla* from time-of-flight measurements on standing trees and density, strain and moisture content measurements from small samples obtained through means of limited destruction, that is through core sample removal. As a logical consequence, the secondary objective of the research was to analyse the variation of each of these wood properties within and between trees from different age classes and genotypes with the use of multivariate ANOVA.

If good predictive models can be developed, part of the main objective is to see if some wood quality problems which arises and increases with age (such as brittle heart and high strain levels), can potentially be identified with measurements on standing young trees between the ages of six to eight years.

2 Literature Review

2.1 Introduction

There is an increasing need and interest in predicting the properties of wood through non-destructive methods, i.e. without having to destroy the living tree or compromise its health or growth. This is due to the fact that lumber with undesirable properties are often graded lower and has less value resulting in final products' lower value and quality. This is especially prominent in *Eucalyptus* sawn lumber as there are various defects which appear after the felling, milling and drying processes. The aim of such initiative is to improve the effectiveness of stands by increasing the value of the lumber produced, and subsequently the value of the end-product obtained from the lumber. Hence, non-destructive testing is applicable in tree breeding regimes where tree breeders need to identify superior genetic material for a breeding population. The value reduction of lumber may be the result of many properties.

The three main defects that will be focused on in this study are splitting, shrinkage and brittle heart, as well as a brief look at other defects such as cell collapse and the various forms of warping (bow, cupping and twist) of the boards. In this chapter, the defects and the parameters that cause and affect them are reviewed. By understanding the underlying issues of the aforementioned defects, an attempt can be made to predict them using possible predictive parameters and tools.

2.2 Defects in *Eucalyptus* wood

2.2.1 Splitting

Log end splitting is a defect which results in substantial material loss when processing logs into sawn lumber. It can only be evaluated after trees are felled, from an age of six years or older once significant growth has occurred to form internal stress in the stem. Splitting is a genetic defect with a heritability range of 0.3 to 0.6 meaning that splitting traits of the parents has a moderate to high influence on the offspring's traits(Barros et al. 2002). This means that a cross of two high-splitting parents will result in a high-splitting offspring and vice versa. In *Eucalyptus* species, this is the result of high levels of growth stress in the tree trunk (Malan, 2008). These stresses are found to be in equilibrium within the standing stem (Malan, 1987; Bichele, 2009) and are released when the tree is felled and the stem is crosscut, causing end splits in the logs which results in lengthwise board splits upon processing (Okuyama et al,2003).

Growth stress in stems are found in either a tensile or compressive state, shown in Figure 2 - 1. Wood cells near the cambium are usually held in tension up to approximately a third of the radius, whilst cells in and around the pith are held in compression (Hardie, 1974; Bichele, 2009). In a standing stem, the gradient of stresses is in equilibrium. Upon felling and crosscutting, the balanced state of the stresses is disturbed by releasing them from equilibrium state. This causes splits and heart checks (Figure 2 – 2) to form as cells which were once in tension begin to shorten and cells in compression begin to lengthen (Kamarudin 2014)

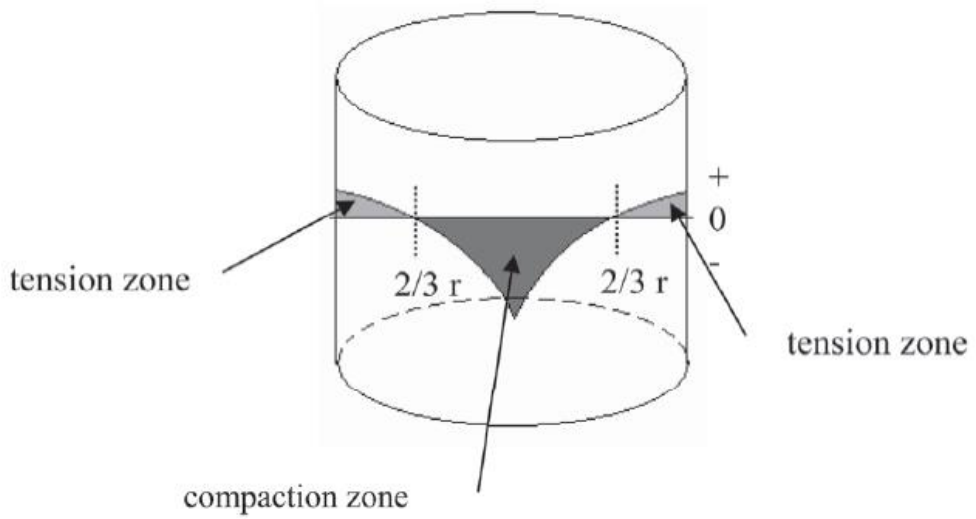

Figure 2 - 1: Distribution of growth stress within the stem (r = radius) (Kubler, 1959).

Upon felling, the longitudinal stresses developed in the stem are converted into radial and tangential stresses at the end of the stem, otherwise known as the cut face. The development of end splits occurs when the tangential stresses exceed the tangential tensile strength (Kamarudin 2014). These stresses cannot be measured directly, however growth strain can be. The stress levels can then be estimated using a function of growth strain and MOE. Strain can be measured upon its release from the tree stem (Raymond et al. 2003). Hence, destructive measurements are the only means currently for evaluating this defect.

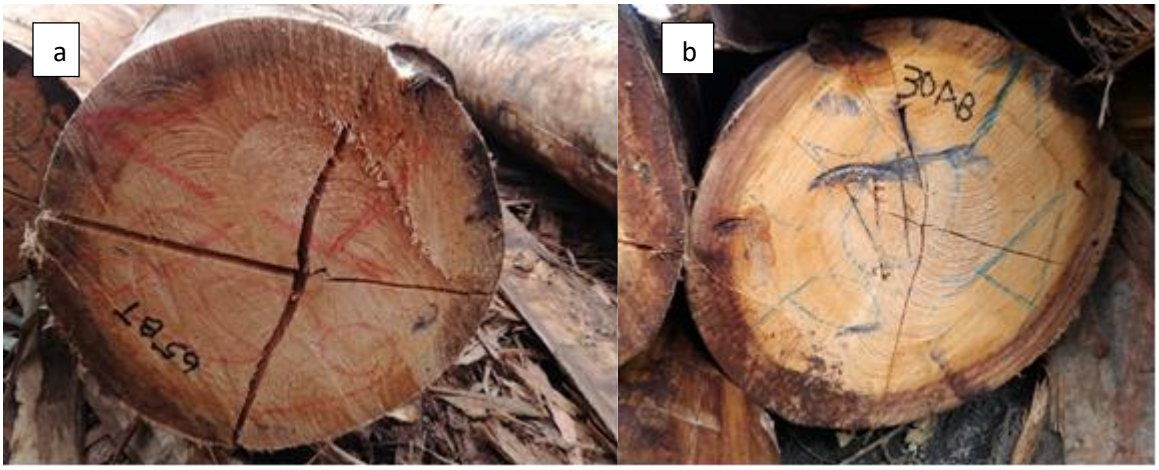

Figure 2 - 2: End splitting after felling (a), formation of heart checks (b).

2.2.2 Shrinkage

Shrinkage of wood is affected by various factors such as density, microscopic structure, moisture, extractives, chemical composition, mechanical stress and microfibril angle (Leonardon et al 2010; Tsoumis 1991). Due to the anisotropic structure of wood, the radial, tangential and longitudinal shrinkage differ. Longitudinal shrinkage of defect free wood is less than 1%, with radial and tangential shrinkage varying between 2-5% for most softwoods (Leonardon et al 2010) and between 5- 13% for some *Eucalyptus* species (Hein et al. 2013).

Shrinkage occurs when the moisture content of the wood is reduced below fibre saturation point. The degree of shrinkage is related to the density of the wood. Wood with higher density tends to shrink more due to the presence of more wood substances and thicker cell walls However, wood with a higher density has a smaller coefficient of anisotropic shrinkage. Hence the microscopic structure of wood is the leading cause for the anisotropic shrinkage. The presence of extractives reduces the shrinkage of wood (Tsoumis, 1991). This is due to the space occupied by the extractives in the cell walls. An increase in extractive content reduces the moisture content. From a chemical composition perspective, lignin has a restraining effect on shrinkage. With an increase in lignin content, the cellulose content is reduced and the shrinkage as well.

Mechanical stresses causing permanent deformation of wood cells also have an impact on the shrinkage of wood. Large compressive stress results in increased shrinkage and large tensile stress results in reduced shrinkage. Even though differential shrinkage is attributed to

the cell wall structure, it is a combination of these factors which determines the magnitude of shrinkage that will occur when the wood is dried (Tsoumis 1991).

2.2.3 Brittle heart

Brittle heart is formed in the centre of the stem and is characterized by the brittleness of the wood and its reduced strength compared to clear wood (Hardie, 1974). It generally occurs in mature trees, and the affected area tends to increase as the tree ages further. Brittle heart is also difficult to detect with the naked eye especially on green cut lumber (Dadswell 1938; Hardie, 1974).

Brittle heart results from an accumulation of compressive forces caused by growth stresses in the stem. As the tree grows, additional layers of cells are added to the outer stem, increasing the compressive forces. When these forces become too great, and exceed the compressive strength in the standing tree, slip planes begin to occur in the cell walls causing brush fractures in the wood in areas of low density. This has a negative impact on the end product and downgrades the strength of the wood where brittle heart is present (Vermaas 2000).

The problem with detecting brittle heart arose from the inability to assess the presence of the cumulative growth stresses at the centre of the stem, and to quantify them as well. It has distinctive low strength properties but is often undistinguishable from healthy, clear wood neighbouring it (Dadswell 1938). Brittle heart is often observed after sawing, and presents a rough, fibrous surface on sawn lumber. Due to these factors, it is difficult to determine if a standing tree has brittle heart present in its stem.

2.2.4 Cell collapse

Collapse is the drastic and permanent deformation of wood cells which results in failure of the wood structure at the cellular level during the drying process when water leaves the wood cells too quickly. This causes ridged surfaces in sawn lumber. These cells lose their natural structure and become deformed and even closed off (Tsoumis1991). It occurs when the stress developed in the cells exceeds the strength of the cell. The stress developed is due to the forces exerted by the water in the wood. Even though these stresses are not strong enough to cause rupture or failure of the wood, it can cause permanent cell deformation, which in turn, weakens the structure of the wood. These stresses can result from poor permeability, and

water becomes trapped in the wood exerting extra pressure on the walls. This phenomenon reduces the integrity of the wood and can present itself as rough and uneven surfaces in sawn lumber. In extreme cases, warping may even occur (Bariska 1992).

2.2.5 Warp

Warp is the deviation of a board from the flat plane, to some areas (corners and edges) being raised out of the initial flat plane. Bow, crook, twist and cup are classified under the term "warp". It is caused by various factors such as spiral grain, uneven drying or sorption, reaction wood and defects such as knots. Tangential and radial shrinkage will occur differently if moisture loss is not uniform or if the moisture content varies within the board, causing warp. This phenomenon is due to the change in internal stresses in the wood when moisture loss or uptake occurs at different rates in the same board (Tsoumis 1991). Warp can lead to reduced mechanical properties, namely MOR and MOE. It can also affect surface quality of sawn lumber (Sepulveda 2001).

2.3 Measurement methods for wood properties

A variety of studies have been conducted and various methods were tested in order to establish a standard test method for the measurement of wood defects. Some of them are listed below.

2.3.1 Growth strain

The following methods have been tested in previous studies to measure growth strain in growing tree's stem.

- CIRAD-Foret method (Raymond 2003; Kamarudin 2014): The CIRAD-Foret strain gauge measures the lengthwise change in the cambium when the growth stress is released from the standing tree via an incision made in the stem of the tree.
- Nicholson Technique (Kamarudin 2014): Two steel studs are glued to the exposed stem surface of the tree, at exactly 50 mm apart and parallel to the grain direction. Two horizontal cuts are made above and below the studs to release the surface strain. The strain can be determined by taking horizontal measurements before and after the cuts are made.

- Strain gauge method (Kamarudin 2014): A strain gauge is attached to the exposed stem of the tree. Growth stress is then released by carving incisions into the stem; above and below the strain gauge for longitudinal growth strain measurements, and to the left and right of the strain gauge for tangential strain measurements.

Each of the three methods for measuring strain are non-destructive as small incisions are made in the stem, however these methods are only able to determine the strain at the periphery of the stem.

2.3.2 Density

The following methods have been tested to determine wood density.

- Basic water displacement (Raymond 2003): Submerge a **wood sample** of known mass in water and measure the change in water level. The measurement obtained from the water displacement (volume) along with the mass of the wood sample are then used to determine the density of the sample:

$$Density = \frac{mass}{volume} \qquad \textit{Equation 1}$$

- Resistograph (Isik 2003): A resistograph drills a needle into the **tree** at a specific drilling rate, and measures the resistance of the wood against the needle to create a drill profile of the tree from which the density profile (from pith-to-bark) can be determined.

- Gravimetric determination (Wessels 2011): For a wood sample of known volume, the density can be determined by obtaining a mass measurement for the sample at certain moisture content. One such method is the maximum moisture method (Smith, 1954) which uses the mass at fibre saturation point and the oven dry mass, as well as the specific gravity of wood

- Computed tomography, CT Scanning (Wessels et al, 2011): Computed tomography scanners can be used to evaluate the density profile of wood core samples. These scanners make use of x-ray imaging to determine various properties including density profiles, presence of decay, knots, checks, grain angle, cell structures, etc.

- Pilodyn wood tester (Shi-jun 2010; Wessels 2011): Determines the density of wood or tests the strength by shooting a spring-loaded needle into the tree. The penetration depth of the needle can then be read off the scale on the Pilodyn tester (in mm). A general sign of lumber strength is minimum penetration of the needle into the wood (15 – 25mm), whereas decaying wood will have higher penetration depths. This depth can also be used

to determine the density of wood indirectly as dense woods have smaller penetration depths.

- X-ray densitometry (Mannes 2007): Makes use of x-ray radiography to produce images on x-ray film, which are analysed using a densitometer to determine the density of 2 mm thick wooden cores ("Silviscan™ Rapid Wood Analysis - Csiropedia").
- Neutron Imaging (Mannes 2007): This technique provides an image of the wood sample produced by neutron attenuation when a low energy neutron beam is passed through the sample via the use of a collimator. The intensity of the beam (grey level values) before and after passing through the sample is used to analyse the sample along with other factors such as the attenuation coefficient, effective attenuation coefficient and the nuclear density.

All methods of determining density are destructive and use wood samples except for the resistance drilling method which is done on standing trees.

2.3.3 Moisture content

- Electrical moisture meters (Tsoumis1991139): use the electrical properties of wood to determine its moisture content, either by electrical resistance or by dielectric properties of wood.
- Distillation method (Tsoumis, 1991:139): uses for samples containing extractives or samples which have been treated. The sample is reduced to sawdust particles and weighed before being placed in xylol and distilled in it for a minimum of 1.5 h.
- Oven-dry method (Tsoumis 1991): this method utilizes the green and oven-dry masses of a wood sample to determine the moisture content, using the following formula:

$$Y = \frac{M_x - M_o}{M_o} \times 100 \qquad \textit{Equation 2}$$

where,

Y = Moisture content (%)

M_x = Green mass of sample (g)

M_o = Oven-dried mass of sample (g)

Similar to density, the methods for determining moisture content require destructive sampling except for the electrical moisture meter which can be used on standing trees.

2.3.4 The SilviScan system

The SilviScan system consists of an integrated set of machines used to evaluate wood properties. The system includes an image analyser, x-ray densitometer, x-ray diffractometer and a scanning spectrometer (SilviScan™ Rapid Wood Analysis - Csiropedia). These machines can effectively measure properties such as cell wall structure, grain direction, density, fibre dimensions, and MOE from wood samples. This technology can be applied in areas of improvement for wood-based products, pulp and paper and tree breeding programmes for better genetics. The downside however is the cost involved in utilizing the SilviScan system.

2.4 Predictive calibrations, properties, and models

Previously, Near-Infrared (NIR) spectroscopy has been used to calibrate regression models for various wood properties. Wood samples in forms of solid cores, strips or chips, or even wood meal, can be used to collect the NIR spectra needed for these calibrations (Thomas, 1994). Properties such as cellulose content, density, MOE, micro fibral angle, and MOR can be determined using NIR (Schimleck et al., 2001). A cellulose content calibration for NIR was developed using 1,800+ samples of *Eucalyptus* wood meal from various species (Downes et al., 2010 & Downes et al., 2012).

Resistance has also been used as a predictor of basic wood density (Isik, 2003). The resistance profile has been used to determine the density profile within the stem without invasively removing core samples. The resistograph has also successfully been used to predict areas of decay in the cross section of standing *Eucalyptus* trees (Johnstone et al. 2007). This study exhibited a good correlation between predicted are of decay and actual area of decay with an $r^2 = 0.7584$.

In 2002, McKenzie and other researchers tried to predict the quality of sawn lumber and veneers of individual *Eucalyptus nitens* trees using increment cores, discs and billets. Properties such as density, MFA, internal checking, sound-velocity, shrinkage and others were measured. This study produced a multiple regression model for MOE as a function of density and MFA with $r^2 = 0.87$ as well as various other correlations and relationships between properties. As well as the model performed, the samples used were obtained from billets and

was viable at an individual tree level, however, such a study is a step in the right direction with regards to predictive modelling and non-destructive testing.

2.5 Conclusion

There are various methods for determining a single property, which have been identified in this review. There are also various properties that can be measured using a single method or technique, however many of these methods are invasive and destructive. The near-infrared spectroscopy and the SilviScan devices which can be used to obtain information regarding MOE, chemical composition, microscopic structure, grain direction and cell collapse require a wood sample obtained destructively. These methods are beneficial for their accuracy and ability to derive significant information from samples but can be costly and destructive nature is not suitable for this study. Many of the defects associated with *Eucalyptus* species appear after processing which can be a major challenge in tree breeding. Hence, better and less destructive means of evaluation are needed for assessing the occurrence of splitting, brittle heart, shrinkage and cell collapse before processing or felling. Indirect and related properties such as MC and density needs to be assessed for relationships that might be useful in predictions, and less invasive methods identified for sample collection for the future success of breeding programs.

3 Methodology

3.1 Sample Material

Based on the data provided by Merensky's Northern Timber's Nursery for all *Eucalyptus* stands, the following list of sampling material was selected:

Table 3 - 1: Group specifications.

Group	Genotype	Age (year)	Seed	Site Index	Spacing (m)	Number of trees	Average Diameter (cm) (Under bark)
YI	*E.grandis*	Young (8)	Improved	51.6	6.05	10	22.5
YU	*E.grandis X uraphylla*	Young (6)	Unimproved	54.8	6.33	10	23.65
MI	*E.grandis*	Mature (12 – 13)	Improved	53.9	6.36	10	34.11
MU	*E.grandis X uraphylla*	Mature (12 – 13)	Unimproved	53.9	6.36	10	31.02
OLD	*E.grandis*	Old (23 – 24)	Unimproved	43.0	5.18	10	35.39
ST	*E.grandis*	Split trial (16 – 17)	Mixed	-	3.5	20	25.54

The significance of the stem groupings was to achieve a material set which included young and mature stems with good genetic traits (*E. grandis*), young and mature stems with less desired genetic traits (*E. grandis X uraphylla*), an older group selected in order to obtain material with brittle heart (which only manifest in older trees), and a group from a previous splitting trial as excess material for assessable properties. The *E. grandis* was genetic material that was improved through a breeding programme based on properties of high volume, low splitting, good stem form and low brittle heart. The E*. grandis X uraphylla* hybrid was not yet improved through a breeding programme although the parent material for the hybrids might already have been selected for good traits. In order to compare the desired properties, groups YI and MI, and groups YU and MU were established from the same seedstock. The site index for these 4 groups were kept as close as possible to avoid unnecessary variability in the properties between compartments. The ST group was selected from a previous splitting trial where a high-split parent was crossed with a low-split parent for the purpose of extra data regarding splitting.

The age groupings of young and mature were to assess whether or not young material could be used to predict the occurrence of future properties in the mature material. The genetic groupings of improved and unimproved were to determine whether there is, in fact, a detectable or measurable difference in the properties, and to possibly compare how the unimproved properties manifest in the young stems as well as its progression over the years. The ideal would have been to have only one species with two genetic origins (improved, unimproved). However, this was not available at the time and therefore the sample selections were done to still be able to test for the age x genotype effect with the intention to obtain a high variation in properties.

3.2 Site information

Sampling was conducted in five compartments shown in Table 3 - 2. The compartments were located in Tzaneen, in the Limpopo Province of South Africa, Figure 3 - 1. In this area the average annual rainfall and temperature are 965 mm and 20.4°C, respectively.

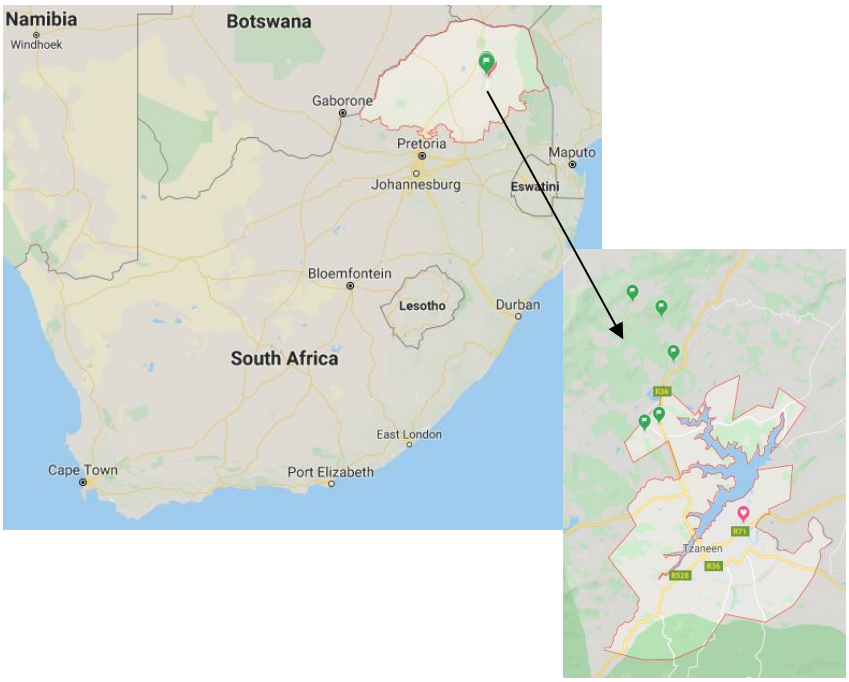

Figure 3 - 1: Sampling locations and sites marked by green pins (Google maps, 2019)

Table 3 - 2: Compartments' locations.

Compartment	Sample Group/s	Co-ordinates	Site Information
F5	YI	23°41'49.8"S 30°05'27.4"E or -23.697159, 30.090948	Slightly sloped terrain
N18	YU	23°46'10.2"S 30°05'54.7"E or -23.769489, 30.098533	Wind swept trees
N21	MI and MU	23°45'54.2"S 30°06'27.0"E or -23.765005, 30.107501	Slightly sloped terrain
G2a	OLD	23°42'20.6"S 30°06'33.8"E or -23.705731, 30.109382	Slightly sloped terrain
A13a	ST	23°43'50.2"S 30°07'01.0"E or -23.730604, 30.116939	Fully stocked compartment

3.3 Sampling Plan

All trees were sampled according to the plan shown in Figure 3 - 2. Sampling on standing trees for the paddle cores were conducted in January 2018, with felling and log processing taking place in March 2018. The paddle core samples for strain were removed at a height of 1 m. Resistance drilling was conducted at a height of 1.3 m in both the N-S, and W-E directions however, the data obtained was not used in this study. Four billets of 150 mm in thickness were also removed at four stem heights, 1.35m, 6.3m, 11.25m and 16.2m for destructive testing of density and MC.

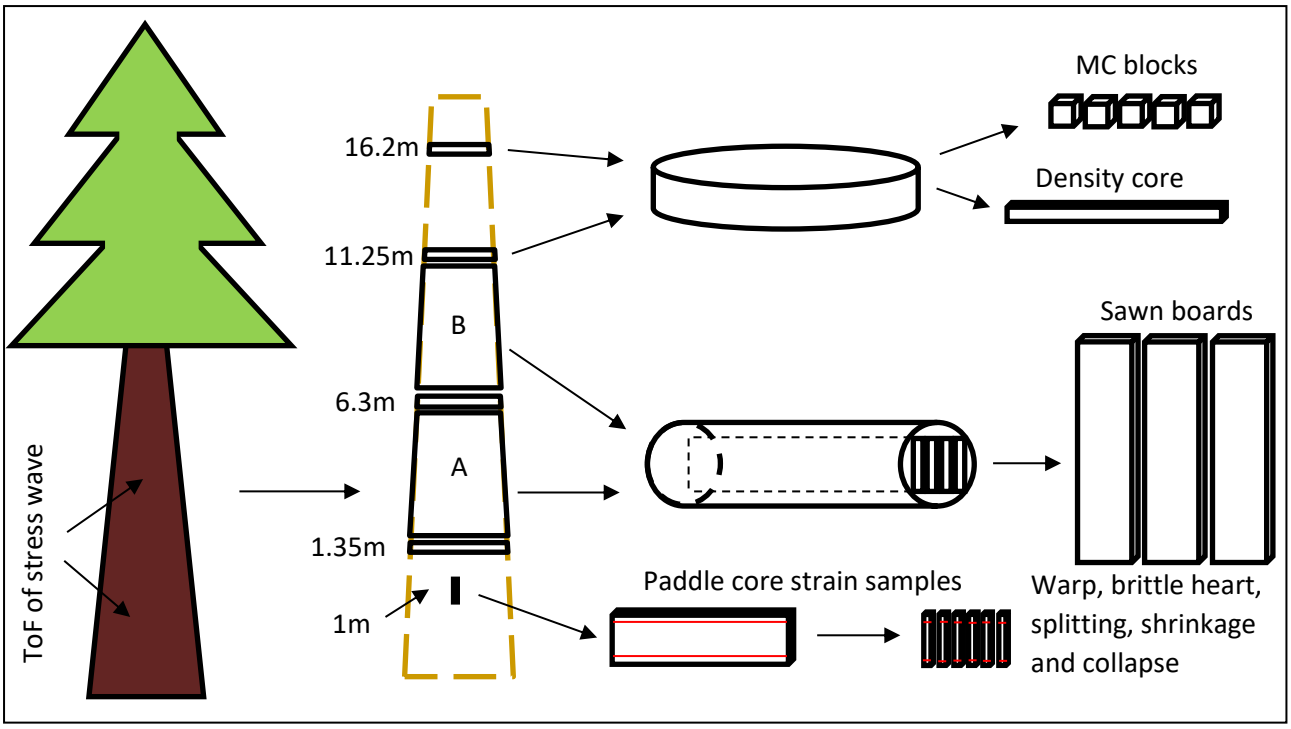

Figure 3 - 2: Stem breakdown, schematic.

Lastly, two 4.8 m logs were removed at heights of 1.5 m (log A) and 6.3 m (log B) for milling into boards. Two cant sawing cutting patterns shown in Figure 3 - 3 were used for the two different log diameter size classes. A pattern of 25 mm x 114 mm boards (mean wet dimensions of 28mm x 120mm) was used for logs with a small end diameter of less than 25 cm, and a pattern of 25 mm X 210 mm (mean wet dimensions of 28mm x 225mm) for logs with diameters greater than 25 cm. With the observed wet dimensions, it can be seen that the boards were severely undersized along the width of the boards, however sizing was not a factor in this study. As is normal with *Eucalyptus* sawmilling, the wet cant width (with target widths of 120 mm and 225 mm) was selected to be roughly 2/3rds of the log diameter. Boards were dried in progressive kilns according to a commercial schedule used at the sawmill. Each kiln consists of 6 phases - the lumber stays in an individual phase for 4 days making the total drying time 24 days. The temperature is only controlled in the last phase where the dry bulb is set to 56 degrees Celsius and the wet bulb to 35 degrees C. The air is then circulated from the last phase through to the first phase where the wet lumber is loaded. The temperature drops progressively from the last to the first phase and the humidity increase progressively making the first, or wet phase act more like a warm-up phase with very little if any drying taking place. The final target moisture content range was 12% - 15%.

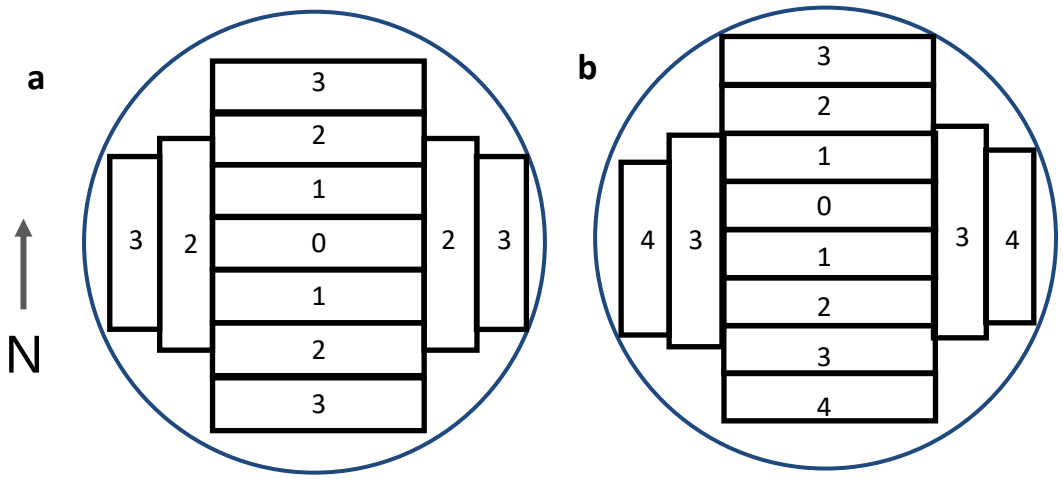

Figure 3 - 3: Sawing pattern used for logs and board position numbering. (Number of boards may differ depending on log size). a) smaller logs with board dimensions of 25 X 114mm, b) bigger logs with board dimensions of 25 X 210mm.

3.4 Properties for evaluation

The relevant properties measured are:

- Time of flight of a stress wave (standing tree stem)
- Longitudinal growth strain (core sample from standing tree stem)
- Splitting (log ends and boards)
- Width and thickness shrinkage (boards)
- Cell collapse (boards)
- Brittle heart (boards)
- Bow, cup and twist were also measured as secondary data to the main defects focused on in this study (boards)
- Density (stick samples from discs)
- Moisture content (block samples from discs)

3.4.1 Density

Wood density was determined using CT Scanning. For this method, a 7 mm X 8 mm **core sample** was taken **from** each of the four **discs** shown in Figure 3 - 4. The lengths of the cores

indicated in Figure 3 - 4 varied between 60-250 mm (in radial direction of the stem), depending on the diameter of the stem at the height at which the sample was removed.

Figure 3 - 4: Density samples (bark-to-pith) for CT Scanning.

The process of CT scanning created a grey scaled 3D image of the sample. The 3D image allowed for any cross section along the longitudinal and horizontal axes, throughout the sample, to be viewed. These grey areas were used to calculate the density at any given point within the sample. Lighter areas indicated less dense material in the sample and similarly darker areas indicated more dense material. After scanning, a sample image of grey values was produced which was used to calculate the density at micrometer intervals using a density equation previously established from a set of calibration blocks (seen in Figure 3 - 5) of the same material as the core samples, with known densities. The equation was obtained for each scan by a simple linear regression, using the known density of the calibration blocks, as well as each block's grey value.

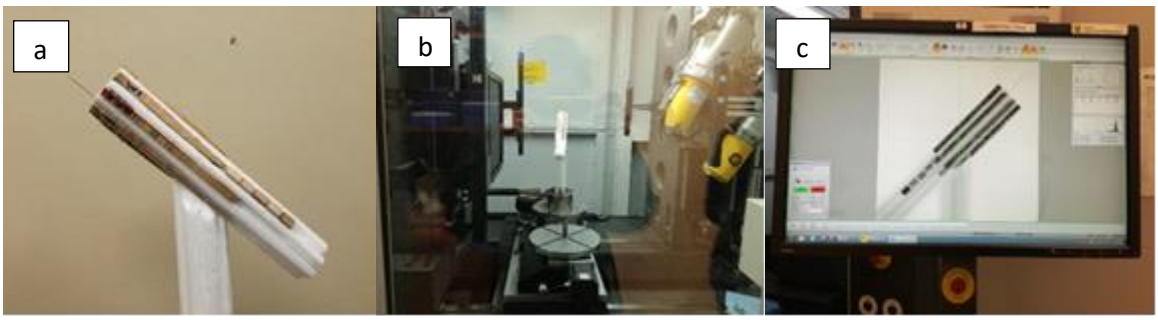

Figure 3 - 5: Density core samples and density calibration blocks in a foam mount (a), samples inside the CT Scanner (b), and grey areas image (c).

To achieve an accurate representation of the density profile, five cross sections were taken across each sample and averaged to obtain a single density profile for the sample. An example of these profiles can be seen in Figures 3 - 6.

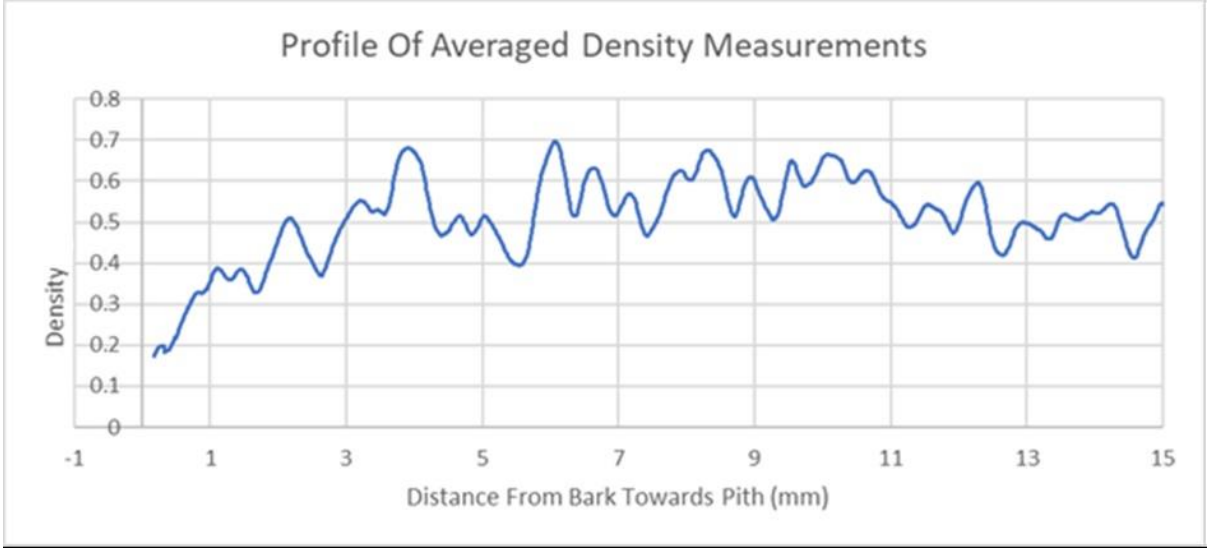

Figure 3 - 6: Profile of averaged CT density measurement (first 15 mm of sample from bark towards the pith) from one disc specimen, measured in g/cm³.

3.4.2 Longitudinal Growth Strain

3.4.2.1 Paddle core strain

In this study, a new method of limited destruction was developed for measuring the strain within the stem of a **standing tree** from pith to bark. This method was developed based on the basic stress strain relationship which results in minute dimensional changes that occur in wood when the stem is cut, and the stress released (refer to figure 2 - 1).

For this method, a rectangular core section with the cross-sectional dimensions of 80 mm X 10 mm (width x thickness), was removed from the stem, with a length reaching the pith (varying from 60 mm to 230 mm) (see figures 3 - 7 and 3 - 9.d). The core was extracted with a battery-operated chainsaw fitted with a custom-made, detachable, locating bracket and a custom-made guiding mount (as shown in figure 3 - 8), to ensure clean and accurate incisions in the stem. Before the core was extracted, markings were inscribed on both faces of each core for strain measurements.

The means of removing a core was fairly simple. The guide rail mount was strapped firmly to the stem of the tree. The chainsaw, fitted with a locating bracket, slotted into two sets of locating holes, used for creating the left and right vertical incisions into the stem, up to the pith. A specialized marking tool was then pushed into each incision, with the help on a guide bar. The tool inscribed the soon to be core with 2 horizontal lines. Once this was completed on both sides of the core, the top and bottom cuts were made to finish off the core. A spacer block which was located onto the guide bar, much like the chainsaw, was used to obtain the correct height for the top horizontal cut. Finally, the core was wedged out of the stem and the sample collection was completed. This process is outlined in figure 3 - 7, with in field photographs of the apparatus and process in figures 3 - 8 and 3 - 9. To ensure consistency, each core was extracted at a height of 1.1m, on the north facing side of the tree stem.

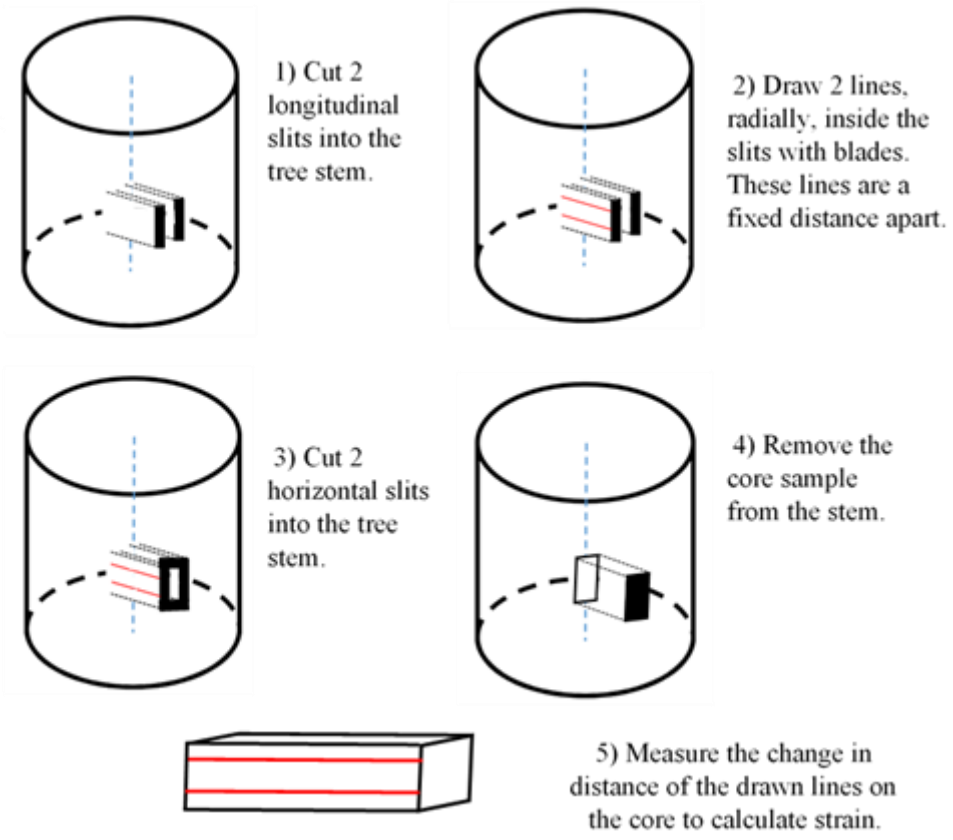

Figure 3 - 7:Diagram of paddle core extraction from tree stem for strain measurements.

Figure 3 - 8: Mount and chainsaw set-up for core removal.

.

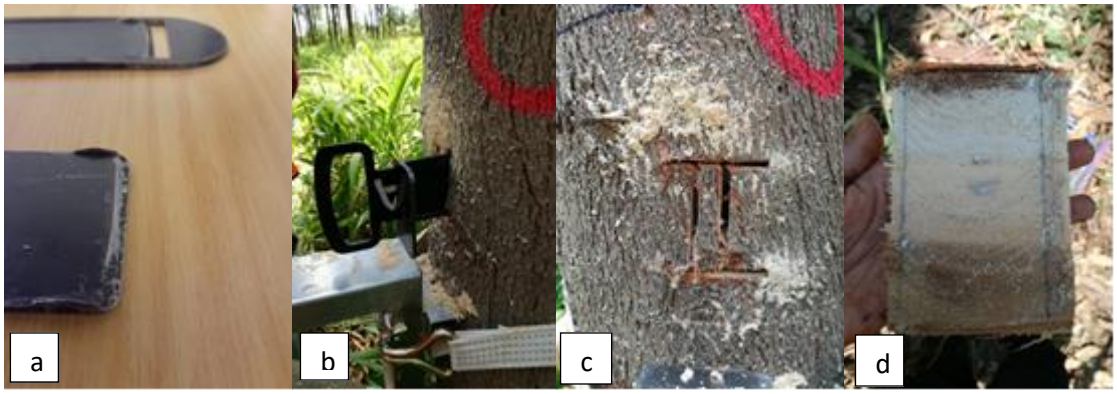

Figure 3 - 9: Marking Tool (a), marking process (b), pattern of all incisions (c), and final core for strain measurements (d).

After the core was removed from the stem, it was cut into 10 mm thick sticks, starting from the bark to the pith (Figure 3 – 10). The distance between the two inscribed markings was measured seven times on each stick using ImageJ, and an average distance for the stick was obtained. This distance, along with the initial distance between the two markings were used to determine the strain in each stick using Equation 3:

$$d = \frac{L_0 - L_1}{L_0}$$ *Equation 3*

where,

d = strain (mm/mm)

L_0 = Initial length measurement (mm)

L_1 = length measurement after releasing the strain (mm)

Figure 3 - 10: Paddle core samples after being cut into sticks for strain measurements.

The marking tool (see Figure 3 - 9, (a) and (b)) broke during the sampling process and was replaced. Since there was a possibility that the outcomes would be influenced by the tool, the tools were treated as a variable during data analysis. The first tool was designated Tool A and the second one Tool B.

3.4.3 Shrinkage

Three width and three thickness measurements were taken along each **board**, before and after kiln drying. Each measured point along the board was marked to minimize errors in the dry measurements data. A digital vernier caliper was used to obtain the measurements (Figure 3 – 11). Shrinkage was then calculated as a percentage of the board's green dimensions, using the following Equation:

$$b = \frac{l_1 - l_2}{l_1} \times 10 \qquad \textit{Equation 4}$$

where,

b = shrinkage (%)

l_1 = green dimension (mm)

l_2 = dry dimension (mm)

Figure 3 - 11: Width and thickness measurements for board shrinkage.

3.4.4 Splitting

3.4.4.1 Log-end splitting

Two types of splitting were measured for this investigation, log-end splitting and board splitting. Board splitting included measuring the split length as well as split width.

Log end splitting was used to calculate an overall splitting score **for the entire tree**. Preferably, these measurements should be done a minimum of 72 hours after the tree has been felled and cross-cut. This allows ample time for the growth stress in the logs to manifest at the log ends as splits. This scoring system used was developed by Conradie (1980), where scores are required for a minimum of four cross-cut faces for each tree, that is two logs. The log end splitting was scored as follows:

- For every crack which extended less than half the log radius – 1 point,
- For every crack which extended more than half the log radius, but did not reach the log edge – 1½ point,
- For every crack which extended to the log edge and had an opening, the width of the opening was measured to the nearest mm and points were awarded accordingly – 1mm = 1 point,
- For any cross cracks which appeared between radial cracks – 1 point.

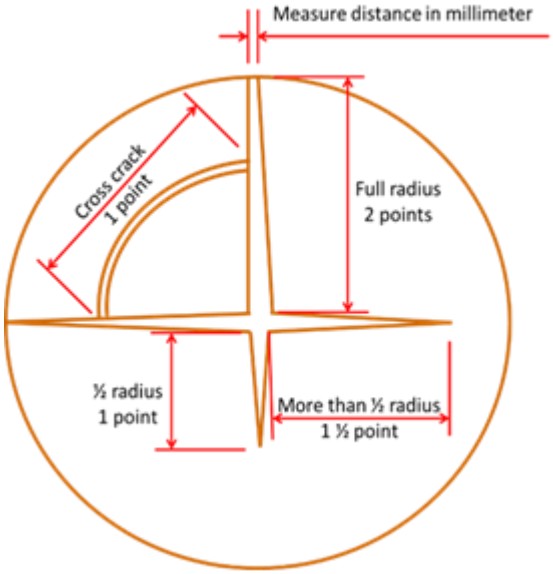

Figure 3 - 12: Visual representation of point allocation for log-end splits.

After each log face had been scored, a **total tree splitting score** was calculated using equations 5 (non-corrected splitting score) and 6 (diameter corrected splitting score).

$$Split_{NC} = 1 \times \left(\sum \frac{1}{2}c\right) + 1.5 \times \left(\sum > \frac{1}{2}c\right) + \sum(Fc, cw) + 1 \times (\sum cc) \qquad \textit{Equation 5}$$

where,

- *Split*$_{NC}$ = Non-corrected splitting score
- 1/2c = cracks less than half the diameter in length
- >1/2c = cracks more than half the diameter in length
- Fc, cw = sum of cracks which extends across the full diameter, and the width of the crack opening, to the nearest mm
- cc = cross cracks

$$Split = \frac{Split_{NC}}{UB\ DBH} \qquad \textit{Equation 6}$$

where,

- *Split* = diameter corrected splitting score
- Split $_{NC}$ = non-corrected splitting score, calculated in equation 5.
- UB DBH = Under bark diameter at breast height

3.4.4.2 Board splitting

Splits were also measured on each individual **board**. The length of the longest split on each end, originating from the periphery of each board was measured whilst green, and after drying with a tape measure, to the nearest millimetre (distance from edge of the board to the red arrow shown in Figure 3 – 13). The width of the split was also measured after drying with a digital vernier caliper, at the split opening, at the periphery (distance between the two blue arrows, Figure 3 – 13).

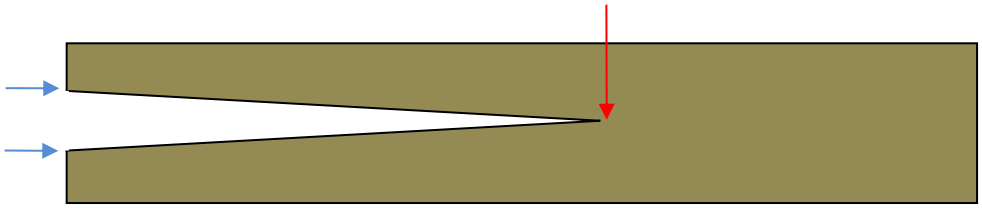

Figure 3 - 13: Board split measurements, length of split from periphery (red arrow) and width of split (between the blue arrows).

.

3.4.5 Brittle Heart

Brittle heart, shown in Figure 3 - 14, was difficult to detect visually on the green **boards**. After drying, the true effects of brittle heart within the boards began to show more prominently hence, it was only measured **after drying**.

Figure 3 - 14: Presence of brittle heart fractures in the board samples.

Brittle heart was determined visually as a percentage of the surface area of each board. Affected sections of the board were marked off using a crayon and the length of each section was measured. The width of each section was allocated either ¼, ½, ¾ or 1 depending on the width of the affected section in relation the board with. This was done for the worse board face, and brittle heart was then calculated as follows:

$$bh = \frac{\left(\sum\frac{1}{4}\times L_1\right)+\left(\sum\frac{1}{2}\times L_2\right)+\left(\sum\frac{3}{4}\times L_3\right)+(\sum 1\times L_4)}{w\times 4800}\times 100 \qquad \textit{Equation 7}$$

where,

- bh = brittle heart (%)
- L_1 = total length of all brittle heart sections expanding a quarter of the board width (mm)
- L_2 = total length of all brittle heart sections expanding half of the board width (mm)
- L_3 = total length of all brittle heart sections expanding three quarters of the board width (mm)
- L_4 = total length of all brittle heart sections expanding the full width of the board (mm)
- w = width of the board

3.4.6 Cell Collapse

Cell collapse only manifests above fibre saturation point (Tsoumis, 1991:154) and it presents itself visually as a washboard effect on the **board** surface (see figure 3 - 15). Hence, for the purpose of measurements from the sawn boards, cell collapse was also scored as a percentage of the surface area, on the worse face of the board.

Figure 3 - 15: Cell collapse creating wash board effect in the board samples.

3.4.7 Moisture Content

Moisture content of the freshly felled wood was determined using the oven dry method. Samples were cut from each of the four **discs** per tree, in 20 mm^3 blocks, from pith-to-bark. The discs removed from the tree were placed in sealed plastic bags straight after cross-cutting the stem for the purpose of preserving the green MC of the samples upon felling. Moisture samples were removed over a 2-week period using a small bandsaw for processing. Due to limited oven space, an average of 20 discs were processed per day and samples were weighed and measured. All remaining samples were left in the plastic bags until they were processed to avoid possible moisture loss due to air drying. The green mass of each **block** was measured before oven drying at a temperature of 103°C for 24hours. After 24hours, the samples were placed in a desiccator until the sample temperature had decreased to approximately that of room temperature. Each sample was weighed once again, and the oven-dry mass was obtained. Equation 2 (see chapter 2) was then used to calculate the green moisture content of each sample. The disc samples were then related to the boards using the distances from pith to bark, and board and MC sample block positioning. Each board, therefore had an MC value linked to it of the wood as it was on the day of felling. Disc A samples were related to log A, and disc B samples to log B.

3.4.8 Time-of-Flight measurements

Stress wave acoustic flight time measurements were obtained using the Fakopp, Tree Sonic microsecond stress wave timer. For this method, two transducers were inserted into the stem of the **tree**, approximately 30 mm deep and 1m apart from each other. A stress wave was produced by knocking the transmitting transducer, and the transit time for this wave to reach the receiving transducer was recorded. Measurements were taken on the North and South

facing sides of the tree stem and averaged to obtain a singular transit time for each tree. The stress wave velocity (SWV, in m/s) can then be calculated as follows (Grabianowski 2006; Shi-jun 2010):

$$SWV = \frac{Distance\ between\ transducers}{transit\ time\ (in\ \mu s)} \qquad \textit{Equation 8}$$

Figure 3 - 16: Measuring time of flight properties with the Tree Sonic microsecond stress wave timer.

4 Results and discussion

The results reported in this chapter were analysed using RStudio statistical software as well as StatSoft Statistica. This chapter is divided into three main sections: (1) Analysis of the effect of grouping (age and genetics), height (log), and board position on each of the main properties namely split length and width, brittle heart, cell collapse, width and thickness shrinkage and density, with warp, ToF, MC as secondary properties; (2) Correlation analyses between the measured properties; (3) Predictive modelling of the main properties from the non-destructive standing tree measurements per age group.

The multivariate ANOVA analysis was conducted to understand the occurrence of each property within the six groups (YI, YU, MI, MU, OLD and ST), across the tree diameter at four different board positions (zero, one, two and three), and at two tree heights (log A and log B). All significant parameters are highlighted in green for easy identification. Where larger diameter logs had additional boards outside of the given zero to three range, these boards were analysed as part of position three, to include the highest possible percentage of the observed data in the analysis. Furthermore, properties could also be analysed across age groups (young, mature, and old) and genetic groups (improved and unimproved) if needed.

Even though analysis of the within and between tree property variations was the secondary objective of this study, it will be presented and discussed first, for a better understanding as to how the properties affected the developed predictive models.

4.1 Property Variations

4.1.1 Split length

For the total of 939 boards, mean split length per board was analysed as the dependent variable with groups, board and log positions as the contributing parameters. End splits were detected in 76.25% of the total boards of N = 716, with the remaining 23.75% having no end splitting present (observed as zero). Table 4 - 1 displays the results of the split length analysis.

Table 4 – 1: ANOVA table for the split length.

	Df	Sum Sq	Mean Sq	F value	p-value
Group	5	8459976	1691995	12.756	5.40e-12 ***
Position	3	3796342	1265447	9.540	3.32e-06 ***
Log	1	648468	648468	4.889	0.0273 *
Group : Position	15	1105688	73713	0.556	0.9087
Group : Log	5	1117348	223470	1.685	0.1356
Position : Log	3	275720	91907	0.693	0.5565
Group : Position : Log	15	1615328	107689	0.812	0.6651
Residuals	891	118184530	132643		

The results obtained indicated a high level of significance for the main factors between the groups as well as the board positions both with a $p<0.01$, and a significant difference between the logs with a $p<0.05$, and no significant differences for the interactions. Figure 4 - 1 shows the variation of split length between groups. Letters of significance are labelled above each bar, indicating which of the data sets or groups fall within the same statistical range of each other. Groups showing the same letter have no statistical difference between their datasets such as group YI and YU both being grouped by “a”.

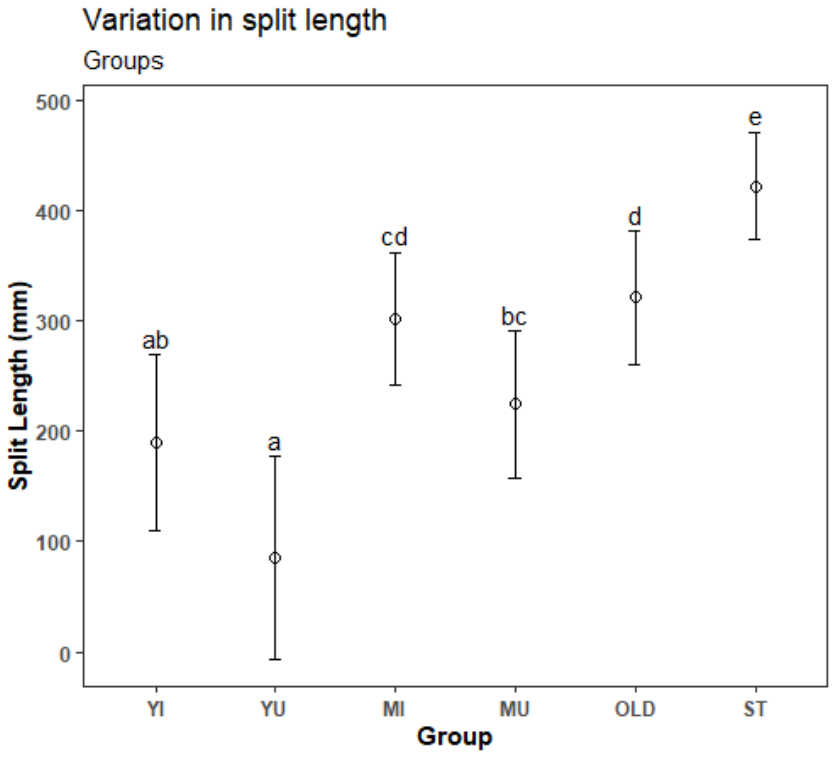

Figure 4 - 1: The variation in mean split length per board across the groups.

According to Figure 4 - 1, as expected, split length increased significantly with age. The two oldest groups (OLD and ST) had significantly longer splits than both the youngest groups (YI and YU) with the OLD group being significantly higher than YI, YU and MU. A study by Biechele et al. (2009) on growth strain exhibits similar results, where growth strain increases significantly with age, between the ages of three to ten years. Malan (2008) also found growth stress to be directly linked to splitting.

The ST group had the highest splitting of all the groups including the OLD group. This can be attributed to the fact the trees in this group were formally part of a splitting trial (refer to section 3.1) wherein different pairs of high and low splitting parents were crossed. However, group YU had the lowest mean splitting and was significantly different to all groups except YI. The results showed that genetic improvement did not have a significant effect on splitting, with improved and unimproved groups having similar split lengths within the same age groups. It should be kept in mind though, that unimproved material was from a hybrid (*E. grandis x uruphylla*) whereas the improved materials was pure *E. grandis* – which means that species itself can possibly also be responsible for the lack of an effect of tree improvement.

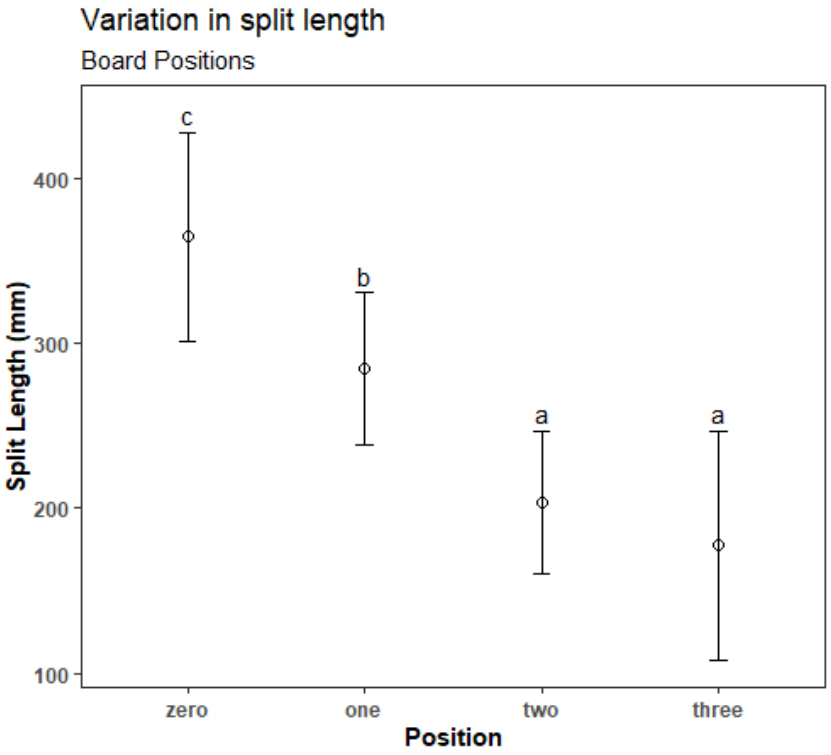

Figure 4 - 2: Variation in split length across board positions, from position zero at the pith to position three at the bark.

Figure 4 - 2 shows that split length was significantly higher at the pith (board position zero) compared to boards at the periphery (board positions two and three). This coincides with previous studies conducted by Priest et al. (1982) where split length decreases significantly from pith to bark. This can be attributed to formation of heart splits originating at the pith as a tensile fracture (Okuyama, 2004) shown in Figure 2 – 2. Board position three had a larger variability since additional boards at positions 4 and higher had also been included into this position category (please see Figure 3 – 3).

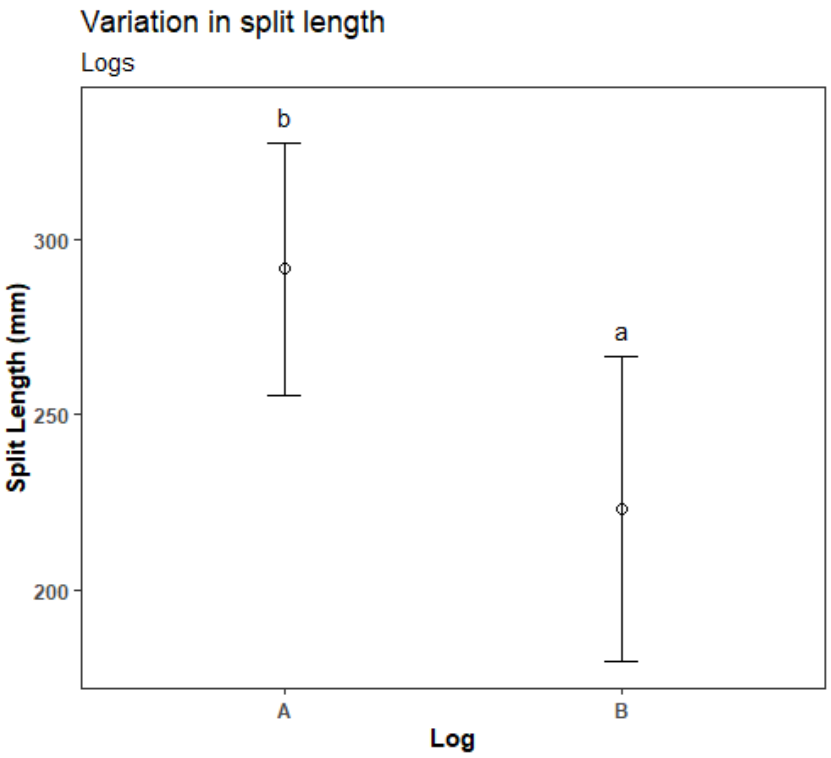

Figure 4 - 3: Variation in split length for logs A and B.

In Figure 4 - 3, it is shown that log A had a significantly higher mean split length per board than log B. This indicates that the split length decreased with height and contradicts the results obtained by Malan (2008) which stated that splitting increases with height. A possible reason is the high presence of brittle heart found in the log A. Figure 4 – 5 showed the same trend for the occurrence of brittle heart between logs A and B, with log A having a significantly higher percentage of brittle heart than log B. The contribution of high brittle heart levels to that of splitting results from the accumulation of compressive forces caused by growth stresses (Vemaas, 2000). This brittle and weakened state of the wood was caused by compression failures as a result of the cumulative stress which exceeded the crushing strength of the wood (Malan, 1984). This was further affirmed by the high correlation between split length and brittle heart and between split width and brittle heart in Table 4 – 15.

Split width yielded similar results to split length, with longer splits having a wider width opening at the board edge. Widths were also larger at the pith than near the bark. This can be seen in Figure 2 – 2, which shows log-end splits tapering in width from the pith, towards the log periphery. This corroborated Okuyama's (2004) study, where the same formation of end splits was found. Split width also had a high positive correlation to split length, Table 4 – 15.

4.1.2 Brittle Heart

Brittle heart was analysed as the dependent variable with sample group, board position and log as the contributing parameters. From 939 boards, brittle heart was detected in only 23.22% of the total boards (N = 218), with the remaining 76.78% having presented no visible signs of brittle heart. Hence, the mean percentages for brittle heart were relatively low (majority being less than 10%) whilst the maximum observed percentage for brittle heart was actually 62%. Table 4 - 2 displays the results of the brittle heart analysis.

Table 4 – 2: ANOVA table for brittle heart.

	Df	Sum Sq	Mean Sq	F value	p-value
Group	5	540	107.9	2.603	0.0239 *
Position	3	6604	2201.4	53.099	< 2e-16 ***
Log	1	248	248.1	5.984	0.0146 *
Group:Position	15	2555	170.3	4.108	2.51e-07 ***
Group:Log	5	202	40.3	0.972	0.4335
Position:Log	3	186	61.9	1.493	0.2149
Group:Position:Log	15	828	55.2	1.332	0.1758
Residuals	891	36940	41.5		

The results obtained for brittle heart indicated a high level of significance for the interaction between the sample groups and board position with a $p < 0.01$. All the individual parameters also proved to be significant, with board position being highly significant ($p < 0.01$), and sample group and log being significant at $p < 0.05$.

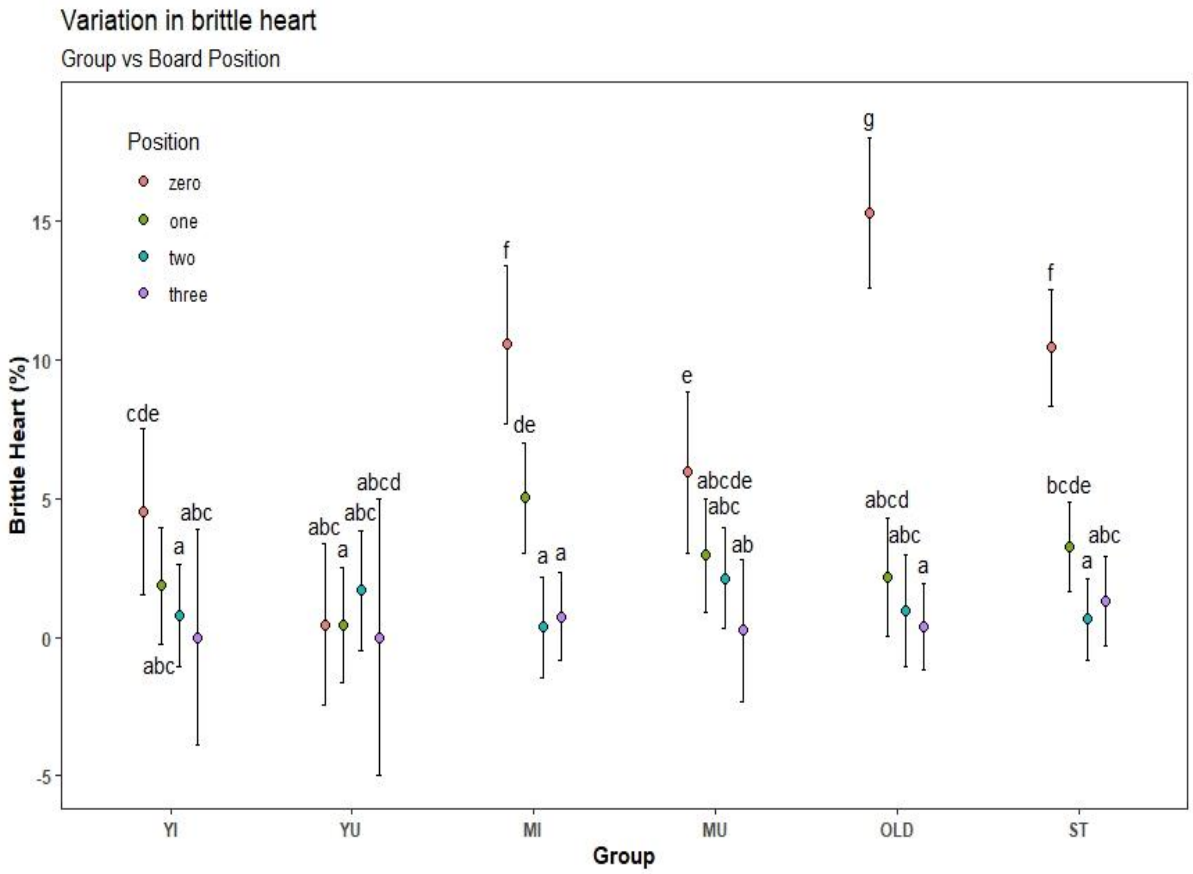

Figure 4 - 4: The interaction between sample group and board position with respect to brittle heart.

Figure 4 - 4 shows the interaction between sample groups and board position with respect to the occurrence of brittle heart. As expected, age played a large role in brittle heart presence. There was a general decreasing trend in the mean percentage of brittle heart from board position zero at the pith, to board position three at the bark. However, in most cases there was no significant difference between positions one, two and three. Groups MI, OLD and ST each showed a significant difference between board position zero and one. This is in agreement with the result of a study conducted by Yang (1995) where it was found that the poor quality wood due to brittle heart was located mainly in the first third of the radius near the pith. Dadswell (1938) also found that the area of brittle heart surrounding the pith increased with age which can be seen in the older groups having higher means for position one than the young groups.

It was also shown that increased age corresponded to increases in the brittle heart in board zero. Despite the fact that groups YU and YI were both classified as “young”, YU was 6 years of age at the time of harvesting compared to 8 years for YI irrespective of genetic classification.

Assessing the groups in order of age (from youngest to oldest), it can be seen that brittle heart started to develop around the 6 year mark (group YU). By age 8, there was significantly more brittle heart at board position zero than at board positions one to three, which were not significantly different from each other (group YI). At 12 years of age (groups MI and MU), the mean brittle heart percentage in board position zero increased substantially along with a slight increase in the rest of the board positions. With group ST at an age of 16 years and group OLD at age 23 years, there was no significant change in the mean brittle heart percentages of board positions one to three, however the mean brittle heart percentage in board position zero continued to increase for the older groups. This corroborates the research conducted by Dadswell in 1938 which stated that brittle heart is formed in the centre of the stem and being more prevalent in older stems. Similar to the splitting results, the genetics did not seem to have a significant effect on brittle heart of board zero in the young group. For the mature group there was a significant difference between improved and unimproved groups in terms of board zero's brittle heart. This corresponded to split length (see Figure 4 - 1) where the MI group had a higher mean split length than the MU group (although the difference was not significant). This apparent superiority of the medium aged and unimproved *E. grandis x urophylla* hybrid to the improved *E. grandis* of the same age in terms of brittle heart and possibly splitting is a significant finding and should be a consideration in terms of species selections for the future.

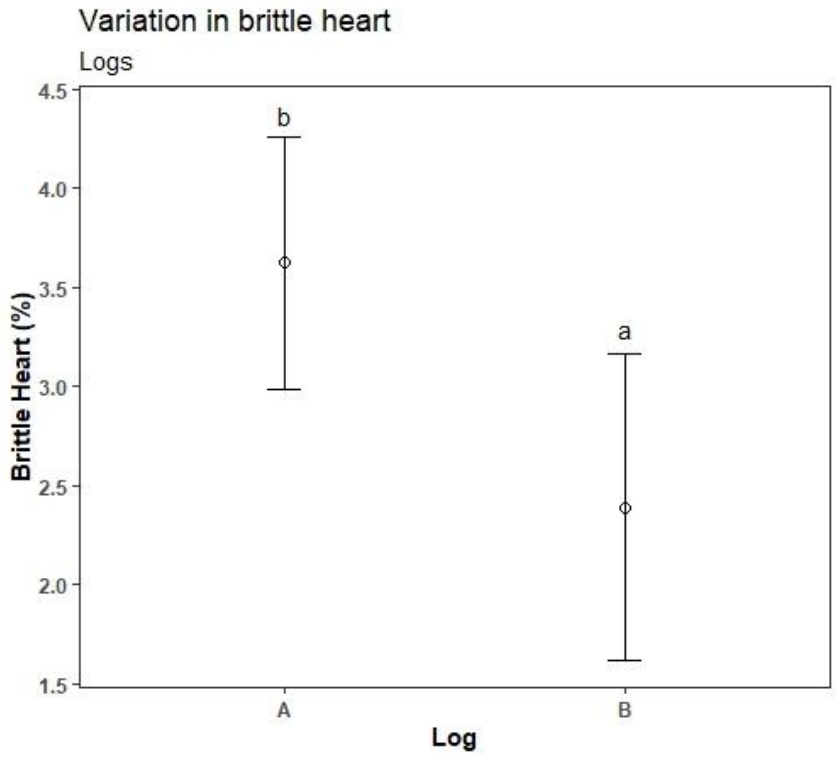

Figure 4 - 5: Variation in brittle heart for logs A and B.

Figure 4 - 5 displays the variation in brittle heart with height. The results showed that the two logs were significantly different from each other with log A having higher brittle heart. Growth stresses are usually larger in older trees and log height also correspond to the age of wood formation. Pith-wood from the butt log forms earlier and is older than pith-wood from higher sections of the stem. Since brittle heart presumably forms due to the compressive growth stresses it follows that butt logs will have more brittle heart than logs higher in the stem. Additionally, according to Dadswell (1938), brittle heart in *eucalyptus* was more widespread in butt logs because the butt log carried more of the tree's weight compared to other logs so it is under a higher amount of stress especially at the pith. Yang (2001) confirmed that brittle heart had little effect on smaller diameter trees. The occurrence of brittle heart decreased with a decrease in diameter and hence height as well. As mentioned previously, the variation of brittle heart with height was similar to splitting results for this study which might be due to the fact that both phenomena result largely from growth stresses.

Appendix B displays an example of a log from the study with severe brittle heart. Within 48 h, the log splitting had increased to such an extent that it was removed from the saw line as it would produce log fragments instead of viable boards for assessment. The brittle heart presumably also exacerbate splitting due to growth stresses since wood strength will be reduced with brittle heart.

4.1.3 Cell Collapse

Cell collapse was analysed as the dependent variable with sample group, board position and log as the effective parameters. 935 samples were inspected and cell collapse was detected in only 14.55% of the total boards, with the remaining 85.45% having no visible cell collapse present. Table 4 - 3 displays the results of the cell collapse analysis.

Table 4 – 3: ANOVA table for cell collapse.

	Df	Sum Sq	Mean Sq	F value	Pr(>F)
Group	5	3739	747.7	9.712	4.80e-09 ***
Position	3	8819	2939.8	38.185	< 2e-16 ***
Log	1	874	874.5	11.358	0.000784 ***
Group : Position	15	6551	436.8	5.673	3.20e-11 ***
Group : Log	5	1798	359.5	4.670	0.000325 ***
Position : Log	3	1829	609.8	7.921	3.23e-05 ***

Group : Position : Log	15	2744	182.9	2.376	0.002304 **
Residuals	887	68289	77.0		

Cell collapse proved to be highly significant for all two-way interactions and all individual parameters. As shown in Figure 4 - 6, the three-way interaction between sample group, board position and log was found to be moderately significant ($p < 0.01$).

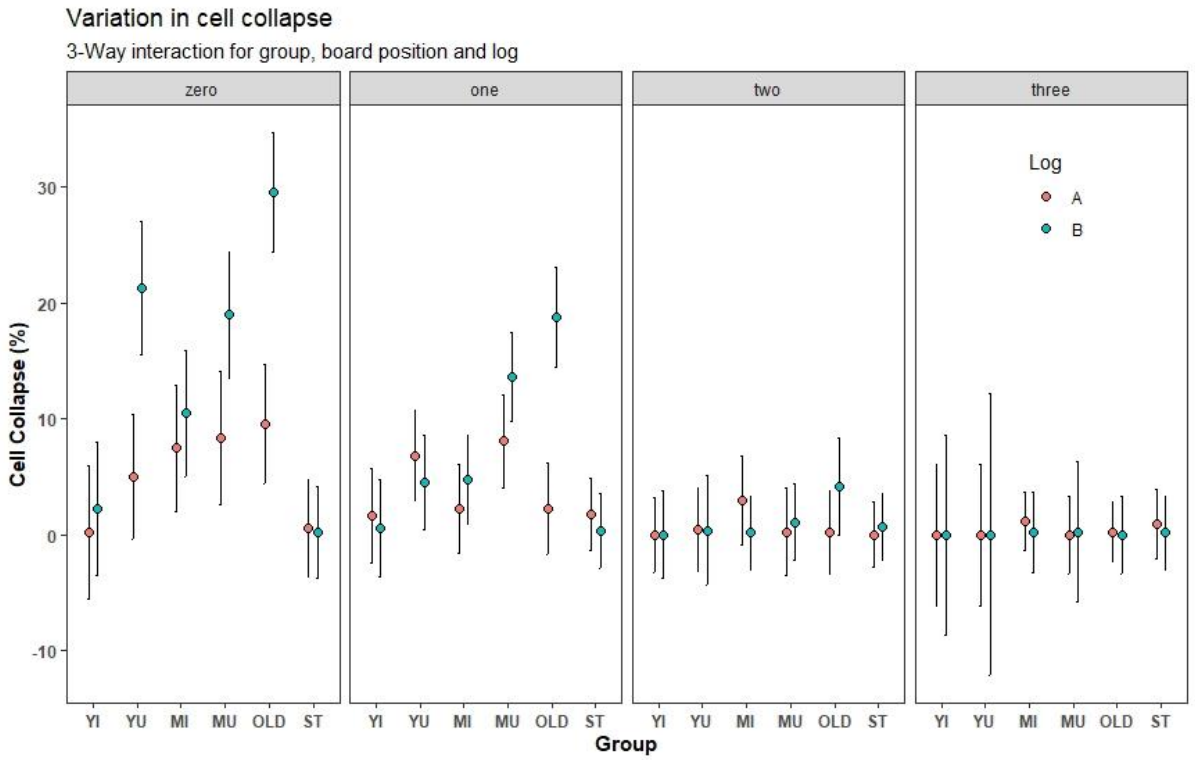

Figure 4 - 6: The three-way interaction between sample group, board position and log with respect to cell collapse. Board position zero is the graph on the left with position three on the right. Appendix A contains all information regarding means, variation and relative grouping.

.

Figure 4 - 6 indicated cell collapse to be concentrated in the pith region at board positions zero and one, similar to the finding by Wu et al (2005), which attributed the increased cell collapse to increased permeability of the cell wall. This is echoed by the results obtained by Gonya (2020) which indicated a significantly higher permeability percentage near the pith region as compared to the regions relating to board positions two and three in this study. However, Chafe (1986) indicated that the collapse increased with distance from the bark to about 85% of the radius where it commenced a precipitous decline towards the pith. AnanÍas et al (2014) found that collapse was more prevalent within the transition zone between the core wood and outer wood. Clarke (1927) also noted that green wood in compression (Figure 2 – 1) is weaker

than in tension and thus results in higher levels of collapse occurring at the core. Board positions zero and one had trends showing increasing cell collapse with age, with the exemption of sample group ST. For board position zero and one, in most cases log B showed a higher percentage of collapse. This contradicts findings made by Purnell (1988) indicating that cell collapse decreased with height. A possible reason for this could be the ratio of heartwood to sapwood. Gonya (2020) found the heartwood:sapwood ratio to decrease with increasing hight. Furthermore, Chafe (1985) found that sapwood had more severe levels of collapse than heartwood in *Eucalyptus regnans*, Board positions two and three have substantially lower percentages of cell collapse, all of which have means below 5%, with 4.12% being the highest of board position two within log B of the OLD group. Furthermore, there was no significant difference between sample groups or log for positions two and three.

4.1.4 Width Shrinkage

Board width shrinkage was analysed as the dependent variable with sample group, board position and log as the contributing parameters. 99.51% of the observed data was used in this analysis, with N = 810. The remaining 129 boards had no observed data as the boards either had irregular shape or were damaged within the drying, transport or handling process resulting in inaccurate measurements. Table 4 – 4 displays the results of the width shrinkage analysis.

Table 4 – 4: ANOVA table for width-wise shrinkage.

	Df	Sum Sq	Mean Sq	F value	Pr(>F)
Group	5	138.5	27.70	17.561	< 2e-16 ***
Position	3	578.8	192.92	122.315	< 2e-16 ***
Log	1	1.5	1.47	0.933	0.33450
Group : Position	15	32.8	2.19	1.388	0.14597
Group : Log	5	26.3	5.25	3.329	0.00555 **
Position : Log	3	10.4	3.48	2.204	0.08622
Group : Position : Log	15	11.2	0.75	0.475	0.95310
Residuals	762	1201.8	1.58		

The results obtained for width shrinkage indicated a high level of significance for the sample groups and board positions ($p < 0.01$). The interaction between the effects of sample group and log also indicated moderate significance with $p < 0.01$.

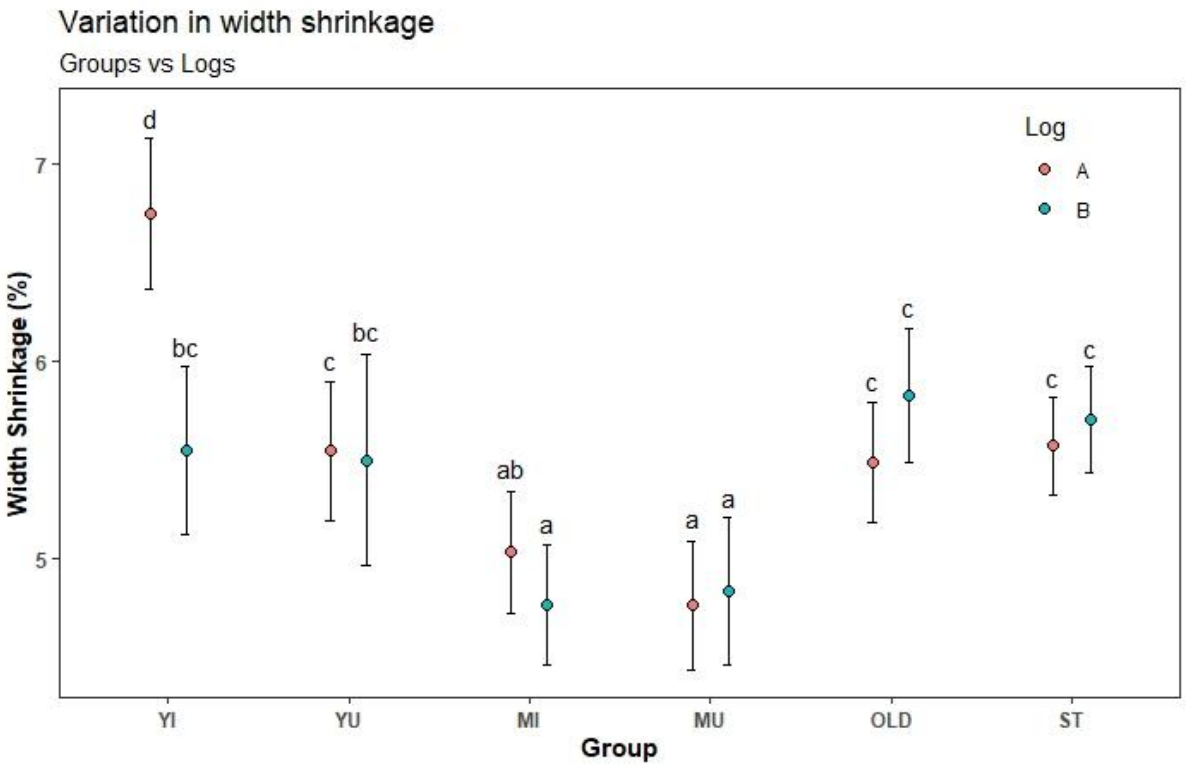

Figure 4 - 7: The interaction between sample group and log with respect to width shrinkage.

Figure 4 - 7 displays the interaction between sample group and log with respect to board width shrinkage. The mature groups, MI and MU had the lowest mean shrinkage along the board width. All the groups had mean shrinkage of less than 6% with the exception of log A in group YI. It had a mean shrinkage of approximately 7% which was significantly higher than any other group. It was also the only age group where the A log had a significant difference with the B log for width shrinkage. The reason for this difference is unclear.

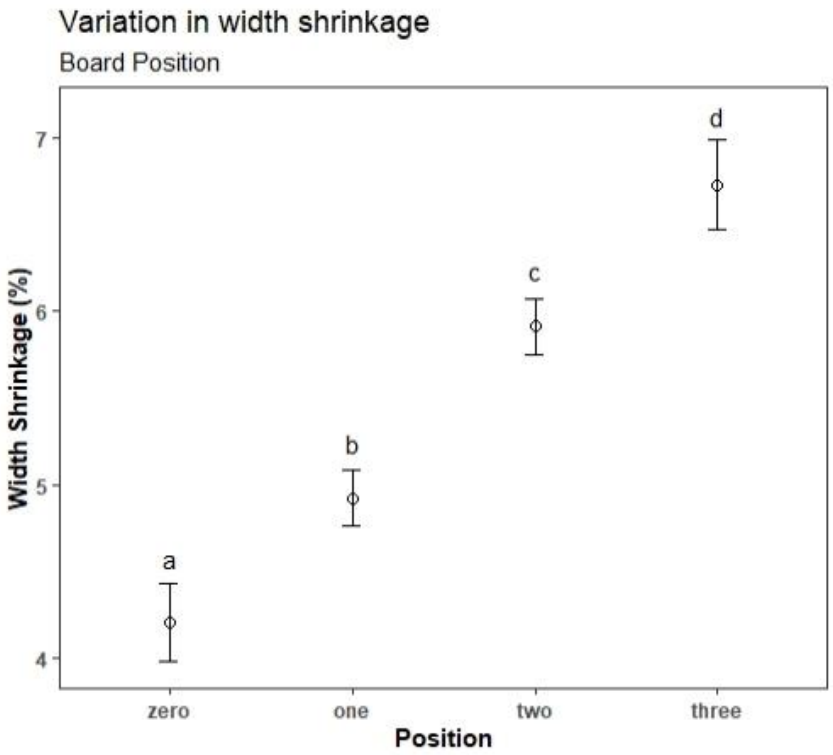

Figure 4 - 8: Variation in board width shrinkage across board positions from pith to bark.

Figure 4 - 8 shows the mean board width shrinkage and variation with the board position. There was a clear pattern of increased shrinkage along the board width from pith to bark. These results were also similar to those obtained by Ekevad et al. (2011) where the width-wise shrinkage of *Picea abies* had an increasing trend from pith to bark. Furthermore, the trend for width-wise shrinkage closely resembles that of density from pith to bark (Figure 4 - 10). Christoforo et al. (2016) explained this relationship by noting that wood with higher density had higher dimensional shrinkage as there is more cell wall material per unit of volume – and it is the cell wall that shrinks when wood dries below fibre saturation level.

4.1.5 Thickness Shrinkage

Thickness shrinkage was first analysed as the dependent variable against sample group, board position and log. The results (Table 4 – 5) produced indicated a level of significance between all three parameters. However, the corresponding graphs were inefficient at displaying the differences. In order to understand and display the results in Table 4 – 5, thickness shrinkage was separated into its age and genetic components and analysed again.

Table 4 - 5: ANOVA table for thickness shrinkage.

	Df	Sum Sq	Mean Sq	F value	Pr(>F)
Group	5	66	13.30	1.705	0.130998
Position	3	371	123.68	15.853	5.03e-10 ***
Log	1	78	77.98	9.995	0.001628 **
Group : Position	15	309	20.62	2.643	0.000638 ***
Group : Log	5	152	30.38	3.893	0.001710 **
Position : Log	3	16	5.31	0.681	0.563771
Group : Position : Log	15	265	17.69	2.268	0.003893 **
Residuals	811	6327	7.80		

The three-way interaction between sample group, board position and log proved to be moderately significant with $p < 0.01$, however, as previously mentioned, the corresponding graph failed to visually show the differences. The interaction between sample group and board position also proved to be highly significant with $p < 0.001$. This was the next suitable option for further evaluation.

Thickness shrinkage was then analysed as the dependent variable with age, genetic groups and board position as the studied parameters. 57.92% of the observed data was used in this analysis, with N = 501. Analysis according to age and genetics instead of sample group eliminated the use of the remaining 364 boards. These boards either fell within the OLD and ST sample groups which were excluded from the age and genetics grouping, or had no observed data as the boards either had irregular shape, or were damaged within the drying, transport or handling process. Table 4 - 6 displays the results of the thickness shrinkage analysis for age and genetics.

Table 4 – 6: ANOVA table for thickness shrinkage.

	Df	Sum Sq	Mean Sq	F value	Pr(>F)
Age	1	0.0	0.04	0.013	0.91034
Genetics	1	21.5	21.51	7.551	0.00622 **
Position	3	148.5	49.49	17.377	9.89e-11 ***
Age : Genetics	1	3.9	3.89	1.367	0.24295
Age : Position	3	0.0	0.00	0.001	0.99997
Genetics : Position	3	10.9	3.63	1.273	0.28291
Age : Genetics : Position	3	22.8	7.59	2.663	0.04741 *
Residuals	485	1381.3	2.85		

The results indicate the board position had a highly significant effect on thickness shrinkage ($p < 0.001$). Also, a moderate significant effect for genetics ($p = 0.006$) and a low level of

significance for the three-way interaction between age, genetics and board position with $p < 0.05$ were found.

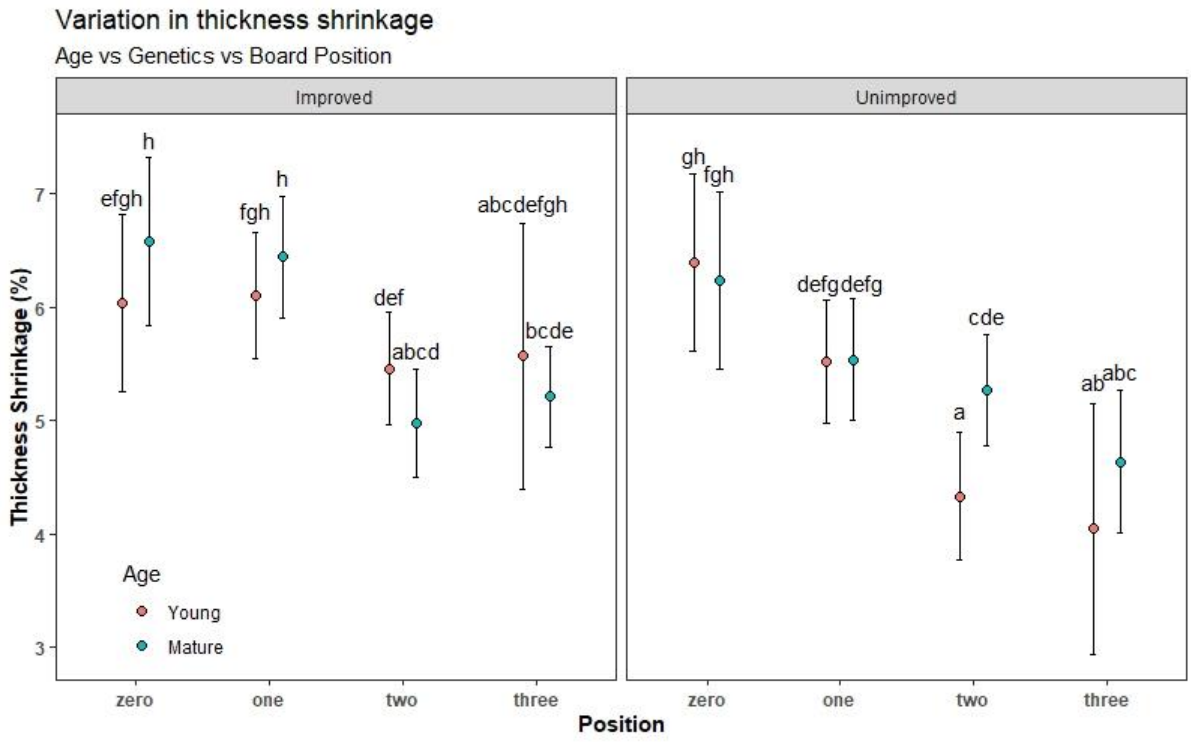

Figure 4 - 9: Three-way interaction between age, genetics and board position with respect to board thickness shrinkage.

Figure 4 - 9 shows the three-way interaction between age, genetics and board position for thickness shrinkage. The improved genetics group showed a higher degree of shrinkage at positions zero and one compared to positions two and three for the mature group. However, there was no significant difference between any of the positions for the young group with improved genetics. The boards from the young group for unimproved genetics mimicked the same trend as that of the mature boards with improved genetics, with positions zero and one having a significantly higher degree of shrinkage than positions two and three. A study by Ekevad et al. (2011) showed a similar decreasing trend for thickness shrinkage from pith to bark of *Picea abies*.

The board positions for the mature boards in the unimproved genetic group differed slightly in significant groupings, whilst still maintaining the general decrease in shrinkage from pith to

bark. This indicates that position zero and one had a higher degree of shrinkage than position three, and positions two and three being significantly lower than position zero. Also, the decreasing rate of shrinkage from pith to bark seems to be higher in the unimproved group.

Figure 4 - 8 shows an increase in width shrinkage from pith to bark; however, Figure 4 – 9 shows a decrease in thickness shrinkage. A similar observation was made by Yamashita (2009) for the *ryuunohige sugi* cultivar in that the trends for radial and tangential shrinkage are different from each other. A possible reason for the difference could be related to how the cells collapsed upon drying. The trend of thickness shrinkage in Figure 4 - 9 is similar to collapse in Figure 4 - 6, where both properties decreased from pith to bark. This trend may have resulted from the cells collapsing in the thickness direction, causing the cells to flatten in the thickness direction while expanding in the width direction. This theory would then agree with the increasing trend for width shrinkage which was also observed by Ekevad et al. (2011), as less collapsed cells near the bark would constitute a higher width-wise shrinkage. Wu et al (2005) documented a similar phenomenon in the trends of cell collapse across the radius. It seems that such collapse will be dependent on the direction of water movement towards the closer open surface and hence thickness-direction collapse. This hypothesis, however, will have to be investigated with a microscopic analysis of collapsed cells.

4.1.6 Density

Density was analysed as the dependent variable with sample group, board position and log as the independent variables. Table 4 - 7 displays the results of the density analysis for 735 samples.

Table 4 – 7: ANOVA table for density.

	Df	Sum Sq	Mean Sq	F value	Pr(>F)
Group	5	0.349	0.0698	7.419	8.64e-07 ***
Position	3	1.836	0.6120	65.019	< 2e-16 ***
Log	1	0.042	0.0417	4.435	0.035565 *
Group : Position	15	0.541	0.0361	3.830	1.37e-06 ***
Group : Log	5	0.201	0.0403	4.276	0.000775 ***
Position : Log	3	0.194	0.0646	6.868	0.000146 ***
Group : Position : Log	15	0.116	0.0077	0.821	0.655095
Residuals	687	6.467	0.0094		

The density results indicated that all the effects and their two-way interactions were statistically significant.

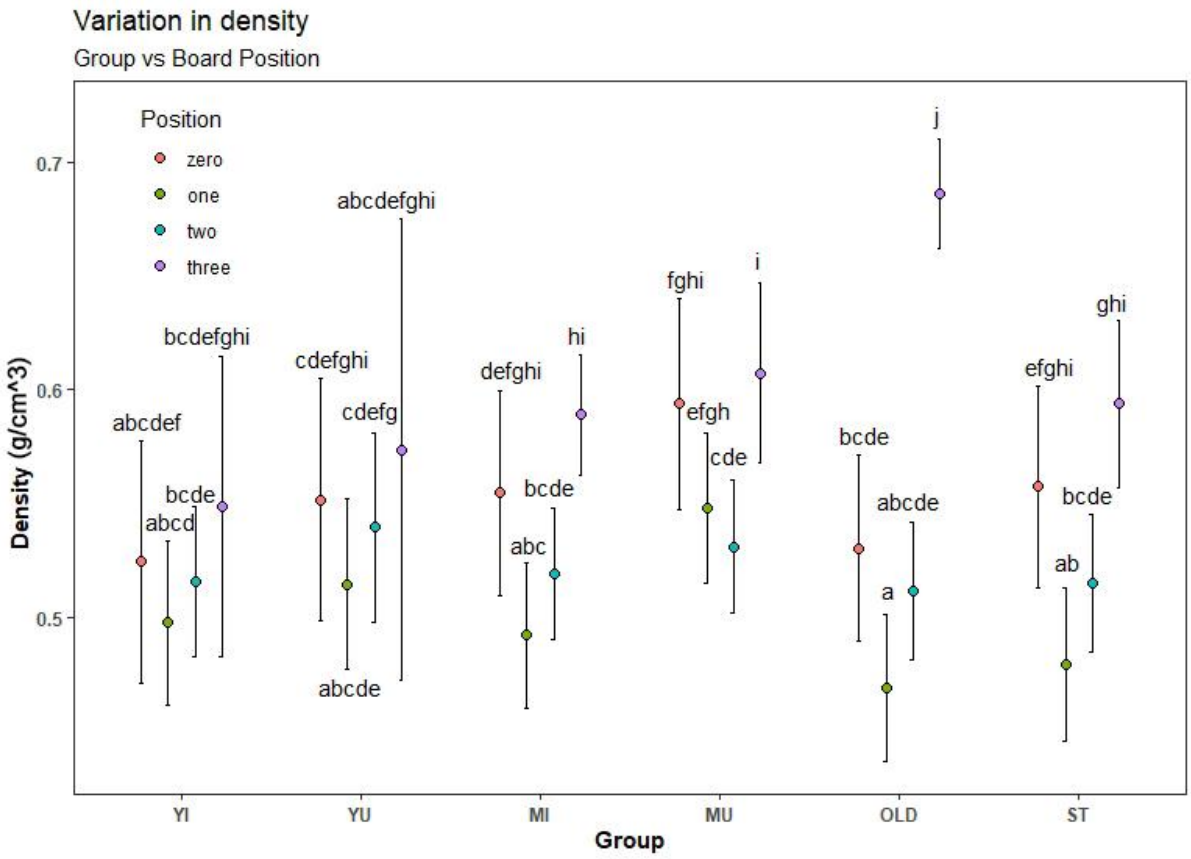

Figure 4 - 10: The interaction between sample group and board position with respect to density.

Figure 4 - 10 shows the interaction between sample groups and board position with respect to density. The general trend showed that density decreased from position zero to one, and then increased from positions one to two to three, indicating a minimum density at position one and maximum at position three. Bhat et al. (1990), Wilkins et al (1991) and Githiomi and Kariuki (2010) reported a similar trend for *Eucalyptus grandis*. A study conducted by Hein et al (2011) shows a similar pith to bark increasing trend for density, with the exception of minimum density occurring at the pith. This trend is evident in all sample groups except MU, which had a minimum density at position two instead. Furthermore, the board positions with maximum density was significantly different to those with the minimum density, with the exception of sample groups YI and YU. It shows that with increased age, the density increased for board position three, also the difference between density of board zero and three increased by age (Kord et al, 2010). For the board positions zero to two, density for the groups had no consistent trend and was generally in the same region. Since board position three also

included boards further from pith, it is to be expected that older trees will be larger and have higher density boards further from the pith. Hence the age effect for the third board position.

4.1.7 Paddle core strain

The strain measurements obtained from the core samples were analysed separately for each marking tool, A and B (marking tools were changed halfway through the process). Since it was found that marking tool A and B gave consistently different results, the data were analysed separately. The data for each tool were analysed across sample groups and board position using ANOVA. Tables 4 – 8 and 4 - 9 displays the results for marking tool A and B, respectively.

Table 4 – 8: ANOVA results for paddle core strain measurements from marking tool A.

Tool A	Df	Sum Sq	Mean Sq	F value	Pr(>F)
Group	2	0.0000763	3.813e-05	3.347	0.0369 *
Position	3	0.0002956	9.853e-05	8.648	1.85e-05 ***
Group:Position	6	0.0001738	2.897e-05	2.543	0.0211 *
Residuals	227	0.0025863	1.139e-05		

The results obtained indicated a high level of significant difference between the board positions with a $p < 0.01$, and slight significance for sample groups and the interaction between position and group with $p < 0.05$.

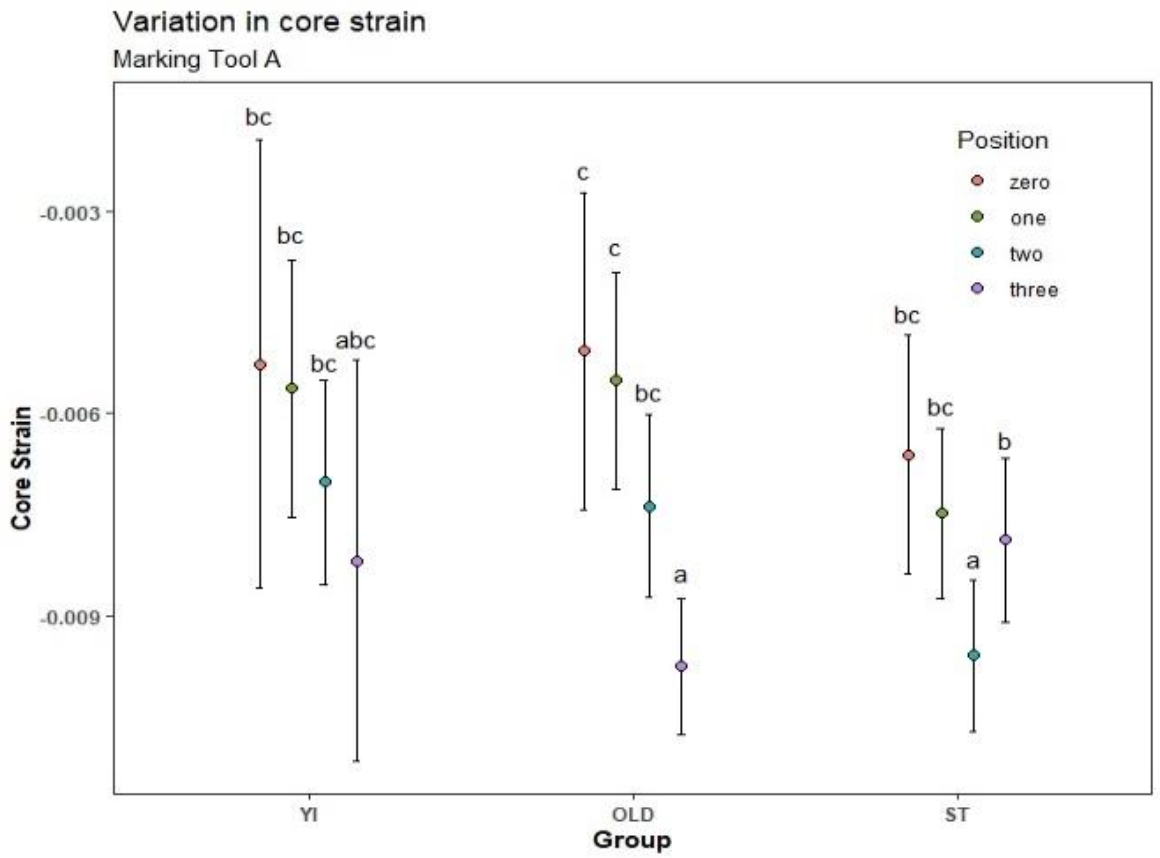

Figure 4 - 11: Variation in strain across board positions for three of the sample groups measured with marking tool A.

Figure 4 – 11 shows a general increase in strain from pith to bark, with groups OLD and ST having a significant difference between the positions with maximum and minimum strain. Both groups had the least amount of strain at position zero with means of -0.00507 for OLD and -0.00661 for ST, and the most strain at position three for OLD with a mean of -0.00975, and position two for ST with a mean of -0.00787. However, according to the literature (Wahyudi et al, 1999), in most cases the strain in the pith is at its peak compared to other parts across the diameter. Strain in the pith is usually compressive and at the bark is tensile (Hardie, 1974; Bichele, 2009). Furthermore, Wahuyudi et al (1999) noted that smaller diameter stems produced much steeper strain curves. This was not the case for results obtained in this study as the OLD group, which had the highest diameter stems, produced the steepest pith to bark strain curve from board positions zero to three. A possible reason for this could be the low level of accuracy of the marking tools. The tools that were used in this research failed to show the compressive and tensive regions throughout the core samples. It showed either completely tensile or completely compression strain. It could be due to the accuracy of the tool or due to the stem eccentricity where the studied trees showed either tension or compression from pith to bark at the side that was sampled (Medhurst et al, 2011). In most case *Eucalyptus*

plantations experience the eccentricity after thinning. It should be noted that the strain amounts were measured in microns, so it is critical to have it measured with high accuracy. The extremely high level of variation was also notable in results which sometimes is an indication of low measurement accuracy. Group YI shows no significant difference between any of the positions. The results also showed no particular significance for age as the same board positions across the different groups produced similar strain means. Wahyudi et al. (1999) observed a similar occurrence in *Acacia mangium* of 4 years and 10 years of age, noting that stem diameter had the biggest effect on strain over age and growth rate.

Table 4 – 9: ANOVA results for paddle core strain measurements from marking tool B.

	Df	Sum Sq	Mean Sq	F value	Pr(>F)
Group	3	0.000386	1.287e-04	6.917	0.000184 ***
Position	3	0.000117	3.900e-05	2.097	0.101740
Group:Position	9	0.000116	1.289e-05	0.693	0.714844
Residuals	210	0.003906	1.860e-05		

Strain associated with tool B is only significant across sample groups with p = 0.000184.

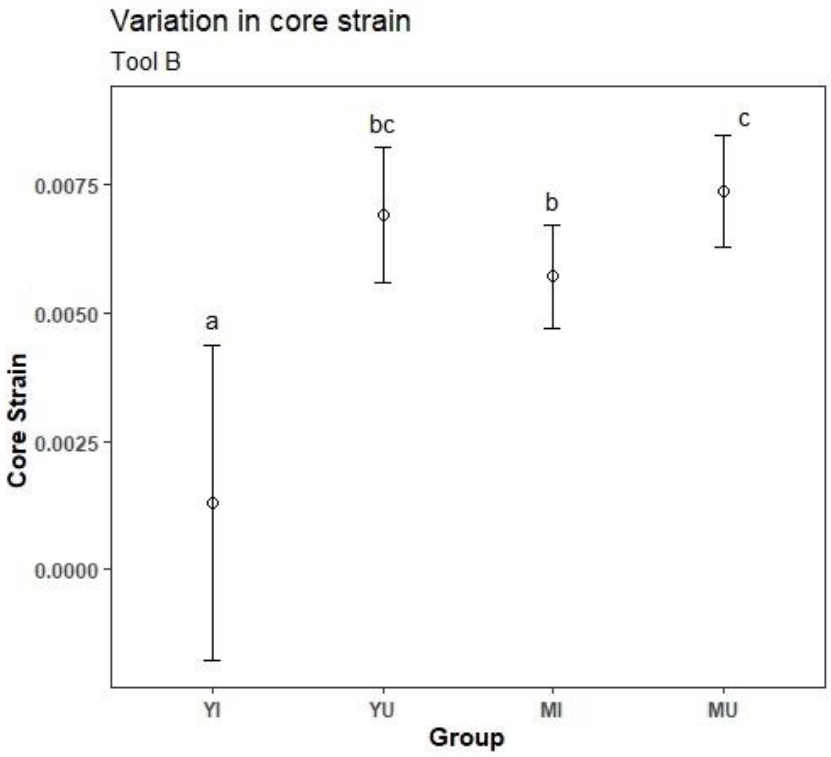

Figure 4 - 12: Variation in strain for four of the sample groups, tool B.

Figure 4 – 12 shows a significant difference between the genetic groups for both ages. The improved groups YI and MI had significantly less strain than the unimproved groups YU and MU respectively. Also, in each genetic group with increased age the strain increased which is in line with the research conducted by Bailleres (1994) as growth stresses are cumulative, with an increase in the stress by the new layers of wood cells added as the tree grows. Another important observation to note is that the wind-swept trees from compartment N18 (Table 3 – 2, which was group YU) produced high results for strain. This may have had an influence on the strain results however this was only seen at the start of the sampling process. Due to the limited time period for sampling, it was not possible to replace this compartment with a different one to fill the criteria for group YU.

4.1.8 Moisture content

MC was analysed as the dependent variable with the independent variables of sample group, board position and log. 94.84% of the data was used in this analysis, with N=900. Table 4 – 10 displays the results. The MC of boards varied between about 75% - 160%.

Table 4 - 10: ANOVA table for MC.

	Df	Sum Sq	Mean Sq	F value	Pr(>F)
Group	5	240856	48171	130.331	< 2e-16***
Position	3	6209	2070	5.600	0.000836 ***
Log	1	94644	94644	256.065	< 2e-16 ***
Group : Position	15	20726	1382	3.738	1.99e-06 ***
Group : Log	5	32160	6432	17.402	< 2e-16 ***
Position : Log	3	16238	5413	14.645	2.63e-09 ***
Group : Position : Log	15	2758	184	0.497	0.942717
Residuals	852	314906	370		

All two-way interaction and single independent variables proved to be highly significant for MC as shown by Table 4 – 10, with $p < 0.001$.

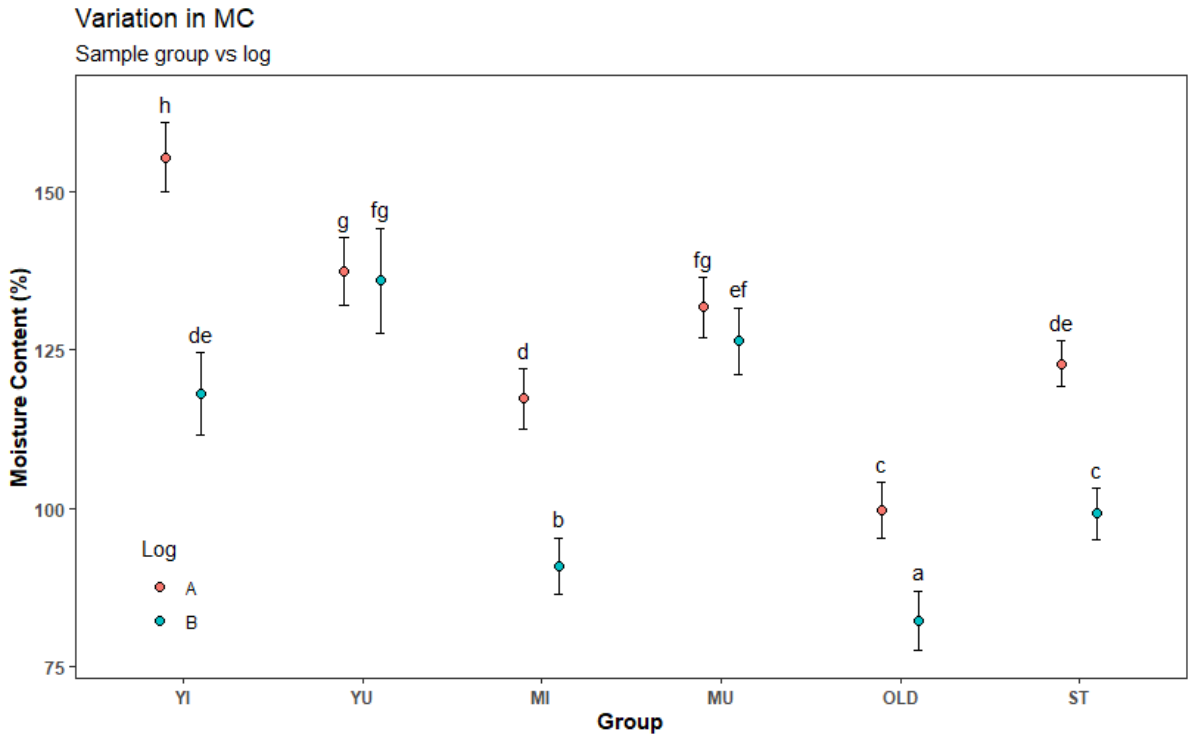

Figure 4 - 13: Variation in MC for sample groups vs log.

Figure 4 – 13 displays the MC variation between logs A and B for all sample groups, where increased age resulted in decreasing MC. It can also be seen that log A had a higher mean MC than log B (Purnell, 1988) for most groups, with the unimproved groups presenting no difference between the two logs.

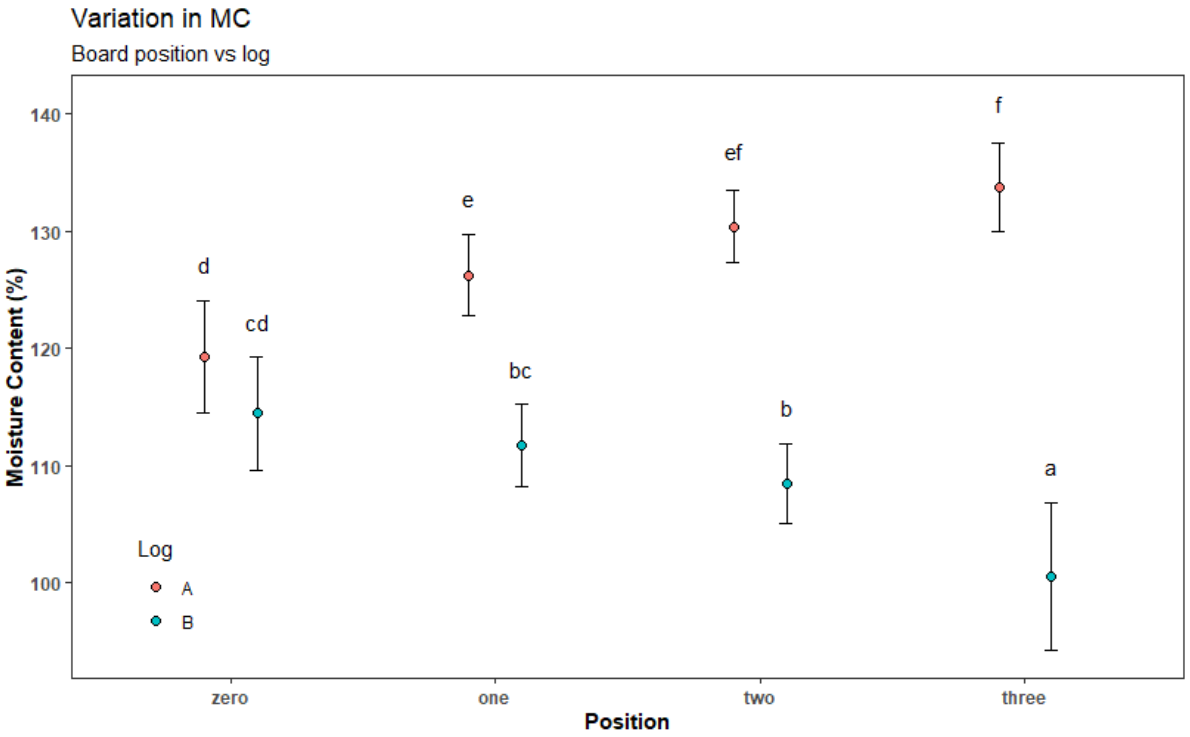

Figure 4 - 14: Variation in MC for board position vs log.

Figure 4 – 14 shows the interaction between board position and log for MC. Similarly to the interaction between sample group and log in Figure 4 – 13, log A had a significantly higher MC mean than log B. Purnell (1988) and Zanucio (2015) noted similar results of decreasing MC with increased height. However, Clark (2000) found that MC increased significantly with height of southern *pine.* Log A also shows that MC increased with radial position from the pith which aligned with MC profiles listed by Tsoumis (1991). This, however, was not the case for log B, where MC had decreased from pith to bark. The reason for these differences is unclear but could possibly be related to some drying out of the smaller discs of Log B outer parts in the plastic bags.

4.1.9 Time-of-Flight

The Fakkop time-of-flight measurements were the only data set analysed at the tree level as opposed to board level. The ToF was related to the boards by assigning the measured ToF from the tree to each board from that tree. ToF was then analysed for its variance across the sample groups alone. Table 4 – 11 displays the ANOVA results obtained. ToF is the time a stress wave travels in one meter of the outerwood of the bottom stem section and is measured in µs.

Table 4 - 11: ANOVA table for ToF.

	Df	Sum Sq	Mean Sq	F value	Pr(>F)
Group	5	193411	38682	101	<2e-16***
Residuals	942	360664	383		

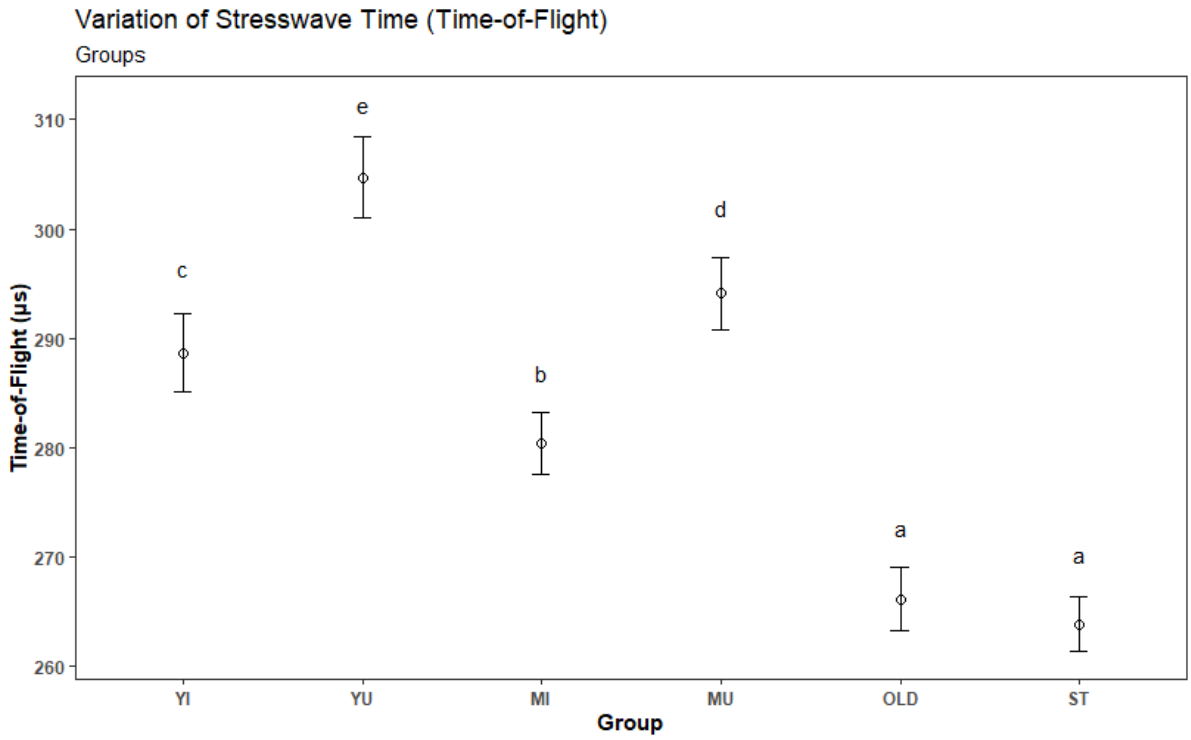

Figure 4 - 15: Variation of stress wave time for groups.

Figure 4 – 15 shows the variation in stress wave times across the groups. The mean time-of-flight decreased with age and genetic improvement. The unimproved groups YU and MU exhibited higher ToF than the improved groups YI and MI. This indicates a **longer flight time** between the transducers and therefore **lower related stiffness or MOE** as well. Furthermore, high stiffness is positively related to strength indicating that poor strength properties could be expected from the unimproved groups. The trend observed in Figure 4 – 15 is however the exact opposite to that of split length displayed in Figure 4 – 1. This is in accordance with Yang & Waugh (2001) which described how high levels of MOE (or low ToF) can indicate high levels of growth stress (or high levels of splitting).

4.1.10 Warp properties

Warp was analysed using 3 variations, bow, cup and twist. Each was analysed as the dependent variable across sample groups, board positions and logs.

4.1.10.1 Cup

98.84% of the boards had measured cupping, which was used for this analysis with N = 938. Table 4 – 12 below displays these results.

Table 4 - 12: ANOVA table for cup.

	Df	Sum Sq	Mean Sq	F value	Pr(>F)
Group	5	0.229	0.0458	3.128	0.00838 **
Position	3	0.165	0.0551	3.764	0.01061 *
Log	1	0.379	0.3793	25.932	4.46e-07 ***
Group : Position	15	0.940	0.0627	4.286	1.03e-07 ***
Group : Log	5	0.118	0.0236	1.612	0.15434
Position : Log	3	0.079	0.0262	1.792	0.14723
Group : Position : Log	15	0.136	0.0091	0.621	0.85950
Residuals	762	11.	145	0.0146	

All single variables proved to be significantly different for cup, with log and the Group:Position interaction both being highly significant with $p < 0.001$.

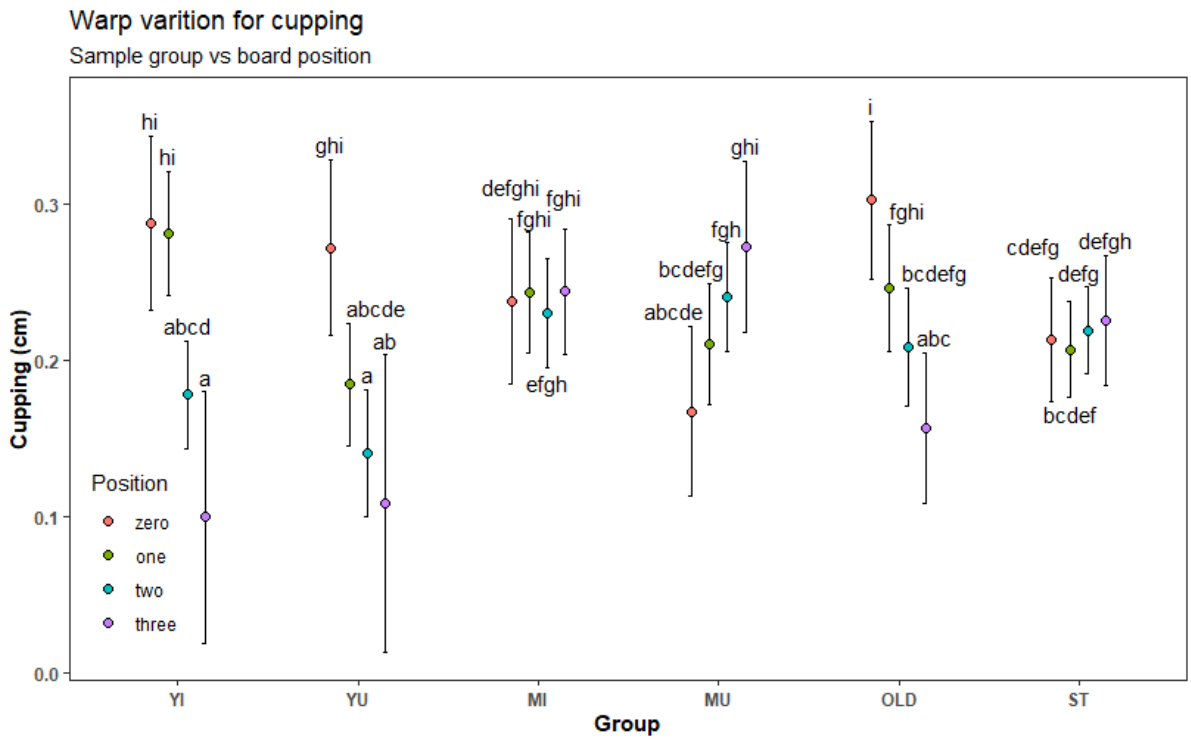

Figure 4 - 16: Variation in cup for sample groups vs board position.

Figure 4 – 16 shows various trends for cupping. Groups YI, YU and OLD had decreasing cup with increased radial position from pith to bark. Group MU showed an opposing trend of increasing cup from pith to bark, whist Groups MI and ST indicated no significant difference at all across the radial positions. The mean cup across all groups fell mainly within the range of 0.2cm – 0.3cm. This means that wet lumber sizes will need to be increased accordingly to compensate the material loss during processing. Such changes should be avoided as it will result in volume recovery losses.

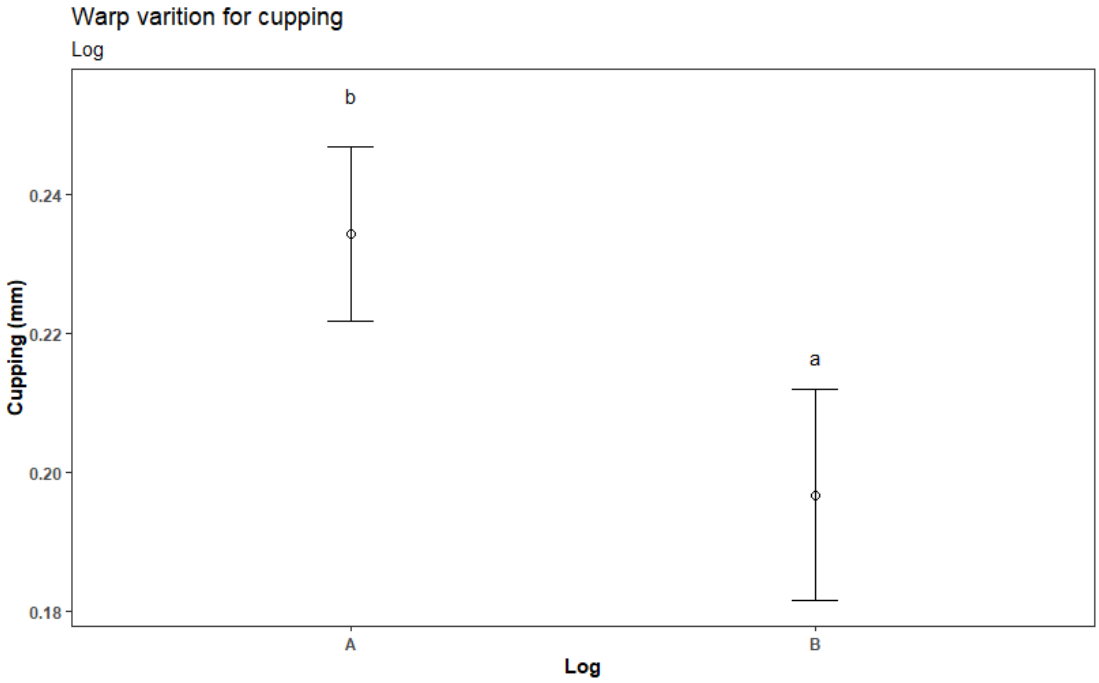

Figure 4 - 17: Variation in cup with log position.

Figure 4 – 17 shows log A had a higher mean for cupping than log B. This could be due to either higher stress levels in the butt log which can cause a higher degree of deformation, or the result of size as log A had more boards of width 210mm than 114mm.

4.1.10.2 Twist

Twist was analysed using 85.67% of the board data with N = 813. The ANOVA results for twist are displayed in Table 4 – 13 below.

Table 4 - 13: ANOVA table for twist.

	Df	Sum Sq	Mean Sq	F value	Pr(>F)
Group	5	3.85	0.7699	2.970	0.011546 *
Position	3	4.41	1.4709	5.675	0.000759***
Log	1	0.25	0.2492	0.961	0.327145
Group : Position	15	9.71	0.6473	2.497	0.001318 **
Group : Log	5	1.12	0.2232	0.861	0.506937
Position : Log	3	0.91	0.3028	1.168	0.320901
Group : Position : Log	15	5.69	0.3794	1.464	0.112337
Residuals	764	198.04	0.2592		

Table 4 – 13 indicates a moderate significance for the interaction between sample group and board position with $p < 0.01$.

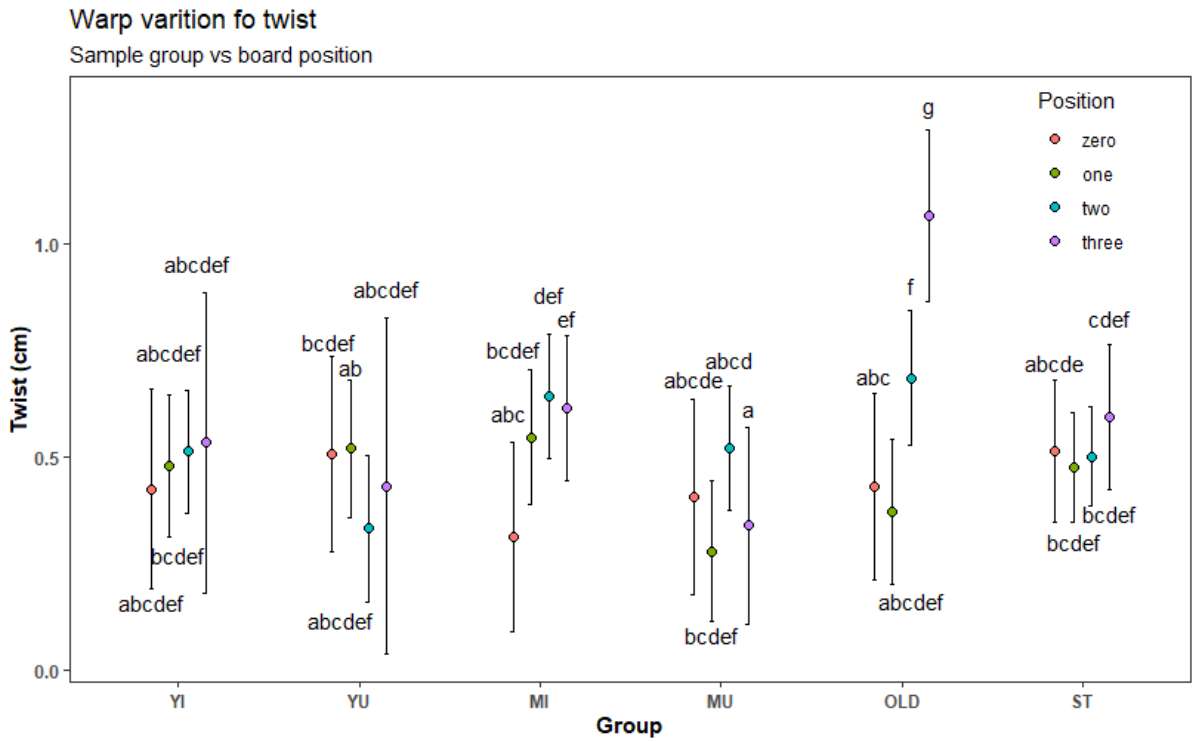

Figure 4 - 18: Variation in twist for sample group vs board position.

Figure 4 – 18 showed relative consistence with regards to twist deformation with majority of the data averaging around 0.5cm. Groups YI, YU and ST had no significant difference in twist from pith to bark, Groups MI and OLD had increasing trends from pith to bark, with board position three of the OLD group having had the highest mean twist over all other groups and positions.

4.1.10.3 Bow

The analysis for bow used 85.35% of the board data with N = 809. The ANOVA results are listed in Table 4 – 14:

Table 4 - 14: ANOVA table for bow.

	Df	Sum Sq	Mean Sq	F value	Pr(>F)
Group	5	2359	472	3.681	0.00268 **
Position	3	38573	12858	100.299	< 2e-16 ***
Log	1	403	403	3.145	0.07655 .
Group : Position	15	3192	213	1.660	0.05403 .
Group : Log	5	928	186	1.448	0.20480
Position : Log	3	419	140	1.090	0.35261
Group : Position : Log	15	1827	122	0.950	0.50718
Residuals	760	97428	128		

Bow showed high significance for board position, with $p < 0.001$, and moderate significance for groupings with $p < 0.01$.

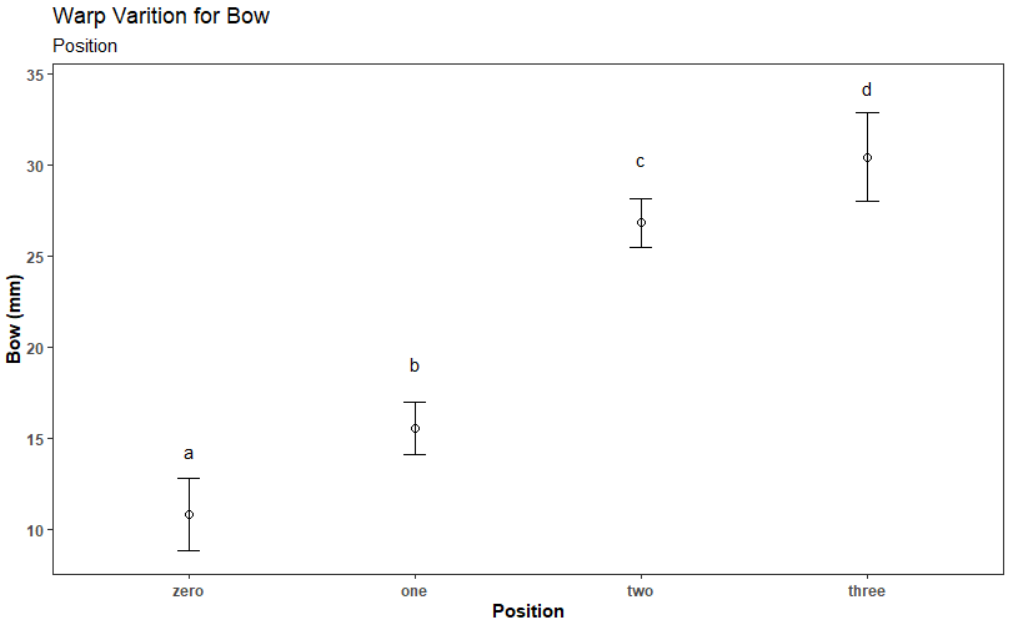

Figure 4 - 19: Variation in bow for board position.

Figure 4 – 19 showed that bow increased with distance from pith, with all positions being significantly different from each other.

The extent of warping can be reduced through uniform drying across the radial, tangential, and longitudinal directions and/or drying under weights as the differences between radial and tangential shrinkage are the main causes of warp deformation (Tsoumis, 1991). This may

improve the dimensional stability of the boards, resulting in less deformation in the final product.

4.2 Property Correlations

Using the correlation matrices function in the StatSoft Statistica programme, the linear correlations between split length, split width, width shrinkage, thickness shrinkage, brittle heart, cell collapse, density, moisture content, strain, stress wave flight time and splitting score was determined. This was only possible after density, MC, strain, stress wave flight time and splitting score data was converted to its board level equivalent to coincide with the rest of the measured data. Table 4 - 15 displays the correlation coefficients along with the corresponding p-values. The marked correlations in green were significant at $p < 0.05$. Positive correlations are identified by positive coefficients, indicating that an in increase in property X will result in an increase in property Y. Likewise, negative correlations are identified by negative coefficients with an increase in property X resulting in a decrease in property Y. A total of 237 observations was utilized for the correlation analysis.

Table 4 - 15: Linear correlation matrix for the mean board data with N = 237.

	Split length	Split width	Width shrinkage	Thickness shrinkage	Brittle heart	Collapse	Density	Moisture content	Strain	ToF	Log splitting Score
Split length	1.0000 p= ---	.5956 p=0.00	-.1648 p=.011	.0478 p=.463	.3821 p=.000	-.0658 p=.313	-.1175 p=.071	-.1400 p=.031	-.1636 p=.012	-.3287 p=.000	.4978 p=.000
Split width	.5956 p=0.00	1.0000 p= ---	-.1495 p=.021	.1500 p=.021	.4587 p=.000	.0070 p=.915	-.1361 p=.036	-.2331 p=.000	-.2343 p=.000	-.3315 p=.000	.3842 p=.000
Width shrinkage	-.1648 p=.011	-.1495 p=.021	1.0000 p= ---	-.0437 p=.503	-.3136 p=.000	-.1054 p=.105	.3688 p=.000	.1206 p=.064	-.1417 p=.029	-.1025 p=.115	.0354 p=.588
Thickness shrinkage	.0478 p=.463	.1500 p=.021	-.0437 p=.503	1.0000 p= ---	.1563 p=.016	.1113 p=.087	-.0369 p=.572	-.0686 p=.293	.0042 p=.949	-.0533 p=.414	.1358 p=.037
Brittle heart	.3821 p=.000	.4587 p=.000	-.3136 p=.000	.1563 p=.016	1.0000 p= ---	.0599 p=.359	-.0722 p=.268	-.1547 p=.017	-.1433 p=.027	-.1313 p=.043	.2715 p=.000
Collapse	-.0658 p=.313	.0070 p=.915	-.1054 p=.105	.1113 p=.087	.0599 p=.359	1.0000 p= ---	-.0758 p=.245	.0509 p=.435	.0171 p=.794	.1544 p=.017	-.1360 p=.036
Density	-.1175 p=.071	-.1361 p=.036	.3688 p=.000	-.0369 p=.572	-.0722 p=.268	-.0758 p=.245	1.0000 p= ---	-.1395 p=.032	.0567 p=.385	-.1812 p=.005	-.0190 p=.771
Moisture content	-.1400 p=.031	-.2331 p=.000	.1206 p=.064	-.0686 p=.293	-.1547 p=.017	.0509 p=.435	-.1395 p=.032	1.0000 p= ---	.3783 p=.000	.4636 p=.000	-.0026 p=.969
Strain	-.1636 p=.012	-.2343 p=.000	-.1417 p=.029	.0042 p=.949	-.1433 p=.027	.0171 p=.794	.0567 p=.385	.3783 p=.000	1.0000 p= ---	.3425 p=.000	.1551 p=.017
ToF	-.3287 p=.000	-.3315 p=.000	-.1025 p=.115	-.0533 p=.414	-.1313 p=.043	.1544 p=.017	-.1812 p=.005	.4636 p=.000	.3425 p=.000	1.0000 p= ---	-.2770 p=.000
Log splitting score	.4978 p=.000	.3842 p=.000	.0354 p=.588	.1358 p=.037	.2715 p=.000	-.1360 p=.036	-.0190 p=.771	-.0026 p=.969	.1551 p=.017	-.2770 p=.000	1.0000 p= ---

As previously mentioned, the latter properties in Table 4 – 15 (MC, strain, ToF and log splitting score) were converted to board level data to coincide with the main defect properties measured on the boards to ensure consistency. Board splitting, brittle heart, collapse and to a lesser extent shrinkage, are the properties with the highest value implications and discussions will centre around these properties.

Split length had positive correlations with split width (r = 0.60), log splitting score (r = 0.5), brittle heart (r = 0.38) and ToF (r = -0.33). This comes as no surprise as split width and length produced similar results and trends. Vermaas (2000) noted that the levels of compressive forces may have influenced the occurrence of brittle heart related to splitting. Similarly, split width also had positive correlations with brittle heart (r = 0.46) and splitting score (r = 0.38), and negative correlations with the stress wave flight time (r = - 0.33). The link between split length, split width, splitting score, ToF and brittle heart is most likely growth stress as high growth stress will result in both splitting, brittle heart and high MOE.

Collapse did not show moderate correlations with any of the other properties – only significant but weak correlations with ToF and log splitting score.

Width shrinkage was correlated to density (r = 0.37) and brittle heart (r = - 0.31). This indicates that samples with high levels of brittle heart presented lower degrees of width shrinkage. A possible link between these two properties could be density. According to Vermaas (2000), samples with high brittle heart tend to have low density. Tsoumis (1991) also states that samples with high density will have a higher degree of shrinkage due to the presence of more woody material. Thickness shrinkage, however, showed only weak correlations to brittle heart and splitting score and none with density or collapse. This result is difficult to comprehend since both density and collapse were expected to influence thickness shrinkage.

It was hoped that the newly developed core strain method will have moderate to strong correlations to properties related to growth stresses such as split length, split width and brittle heart. In fact, the strain had significant but weak correlations with all these properties as well as log splitting score. As discussed previously, this might be due to the marking tool not being accurate enough. Surprisingly the strongest correlations were with moisture content (r = 0.38) and the ToF (r = 0.34). Similar results were obtained in a study conducted by Okuyama (2004)

on longitudinal growth strain as an indicator of heart splits. The difference between the two studies is that Okuyama identified a positive relationship between splits and strain as opposed to the negative coefficients given by the linear correlation in this study. This can be attributed to the tools used for the strain measurements or the method used in analyzing the strain data.

The correlation analyses provided mostly weak or moderate relationships between properties that were expected to have moderate to strong correlations. This has often been the case on studies with *Eucalyptus* species (Chauhan, 2004). The reasons might be due to the variety of factors influencing the wood properties combined with measurement inaccuracies.

4.3 Predictive properties and models

The ultimateobjective of this study was to develop models for predicting splitting, brittle heart, cell collapse, or shrinkage present in sawn *eucalyptus* lumber from non-destructive tree and property measurements. The regression models were built using the linear mixed effects modelling in RStudio, with calculated marginal R^2 as the best model indicator values alongside the predicted vs observed graphs for evaluation.

Models were developed using the full dataset (all trees and boards) as well as separating the dataset into different groups and developing individual models for groups. In general, it was difficult to find models that could predict any of the relevant lumber properties accurately. None of the models on the full dataset proved to be sufficiently accurate, with a few models on separate groups that showed promise.

The data used to obtain the models described below were taken at board, disc and core levels, of groups YI and YU, and converted to a single, common level (board level for this study). This means that models can be used for predictions at different sample levels (board, core or disc) depending on the input level or output requirement. Furthermore, a basic linear regression was conducted between split length and the splitting score method currently in use, to determine if it is in fact a good predictor of split length in sawn boards.

One of the aims of this research was to see whether properties measured on the group of young trees (YI and YU) could possibly indicate the manifestation of problematic lumber

properties in older trees of the same genotype (MI and MU). In other words, to see if some mature wood quality problems can already be identified in young trees. However, given the generally poor relationships between measurables on standing trees and in sawn boards, this part of the research was not successful.

4.3.1 Regression Models

Model 1: Split length

The model with the best marginal coefficient of determination (marginal R^2 = 0.772) was that for split length in the boards of young trees (groups YI and YU). This model is a combined effect of moisture content from the disc level, ToF at tree level and strain measurements at a core level, all converted to board level as required by the split length output, with N = 56. The model is presented by equation 9.

$$SL = -374.2MC - 182.3TOF - 6106000CS + 1.198\,(MC \times TOF) + 41460\,(MC \times CS) + 19830\,(TOF \times CS) - 135\,(MC \times TOF \times CS) + 57140 \quad \textit{Equation 9}$$

Where:

SL = split length (in mm)

MC = moisture content (%)

TOF = time of flight (µs)

CS = strain (unitless)

This model was further evaluated by analysing the predicted vs observed graph shown in figure 4 - 20. The marginal R^2 for model 1 indicated a good correlation between the model and the observed data.

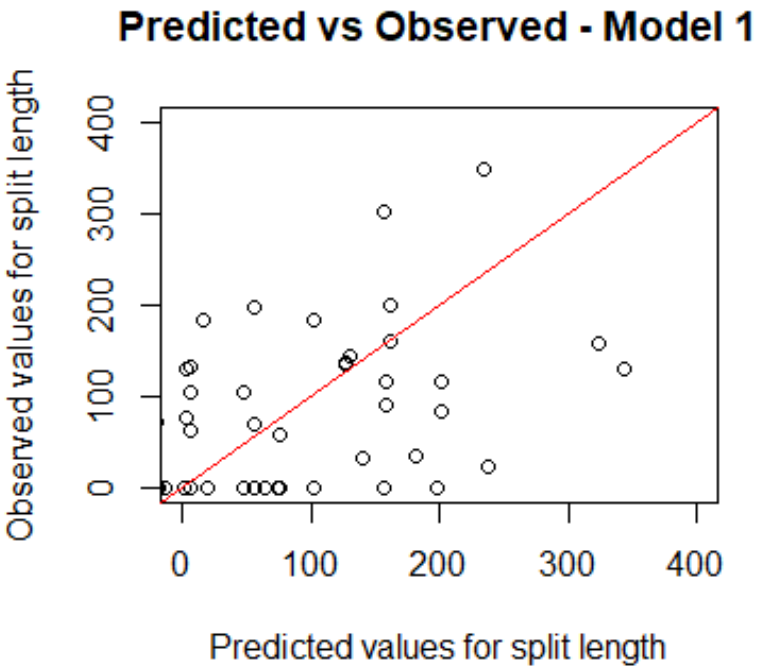

Figure 4 - 20: Predicted vs Observed graph for split length – Model 1.

Model 1 Sensitivity Analysis

A sensitivity analysis was performed for the model predicting split length in equation 4-1. It was conducted over the range of observed data from the 5th to the 95th percentile. This was done by changing each property within the model from the 5th to the 95th percentile whilst keeping the other properties constant at the mean of the observed data set. The predicted range for the dependent variable was then compared to the range of the observed dependent variable (split length in this case) for each property to determine the effect of each variable on the output of the model. Table 4 - 16 displays the results of the sensitivity analysis conducted on model 1.

Table 4 - 16: The influence of each variable upon split length in Model 1.

Independent variables	Influence (%)
MC	30.67
CS	11.06
TOF	37.57

According to table 4 - 16, acoustic properties (TOF) had the biggest influence on the dependent variable outcome with 37.57%, followed by moisture content with 30.67% whilst strain only accounts for 11.06%. Each of the independent variables had a negative effect on split length, where split length decreased which an increase in any of the variables.

Valencia et al (2011) found longitudinal growth strain to be significantly and positively related to log end splitting. A linear mixed model fitted to the data for strain produced low to moderate R^2, ranging from 0.01 to 0.48 depending on the relating trait (Appendix C-1, C-2).

Both these models proved that longitudinal growth strain could potentially be a good predictor for log and board splitting, if measurements are obtained with the utmost accuracy and are combined with other influencing factors such as diameter. By comparing Figures 4 – 1 and 4 – 15 (split ANOVA and ToF anova), it is easy to see why ToF had the biggest influence on the model, given the relationship ToF and split length (Yang & Waugh, 2001). ToF is related to stiffness and strength of wood. In model 1, higher ToF is related to lower split length. Higher ToF would present lower stiffness wood that was linked to higher growth stresses in previous studies (Yang & Waugh 2001). Also, in model 1, higher MC was related to lower split length. The influence of MC is not obvious to explain although it could be related to other properties such as sapwood presence or density, which might be the actual drivers of splitting behaviour.

Model 2: Cell collapse

The model with the second-best coefficient of determination of marginal $R^2 = 0.332$ was that for cell collapse in young trees. This model included moisture content, density, acoustic and strain measurements as the parameters used to predict collapse. The model formula is presented by equation 10.

$$CC = -83.55MC - 18720Dens - 35.87TOF + 143.9(MC\ X\ Dens) + 0.2757(MC\ X\ TOF) + 62.39(Dens\ X\ TOF) + 265.8(MC\ X\ CS) + 36500(Dens\ X\ CS) - 81.85(TOF\ X\ CS) - 0.4762(MC\ X\ Dens\ X\ TOF) - 423.9(MC\ X\ Dens\ X\ CS) + 10800 \quad \textit{Equation 10}$$

Where

CC = cell collapse (%)

MC = moisture content (%)

Dens = density (kg/m³)

ToF = time of flight (µs)

CS = strain (unitless)

The marginal R^2 indicates a moderate to poor fit of model 2 to the observed data. A sensitivity analysis was not conducted for model 2.

A study by Wentzel-Vietheer and other researchers (2013) using NIR spectra developed a model for predicting tangential shrinkage at 12% MC (Appendix C-3). This model accepted the parameters of NIR-predicted cellulose content and NIR-predicted MOE as the independent variable. It explained 64% of the variation in tangential shrinkage when applied to the weighted data and 35% when applied to the entire data set. The predicted shrinkage successfully indicated areas of non-recoverable collapse in the wood core samples.

The Wentzel-Vietheer model and the model produced from this study uses different properties to predict the occurrence of shrinkage and cell collapse. It was also more effective at identifying cell collapse, proving that NIR spectra is a good method for obtaining valuable information regarding collapse, as opposed to the methods in this study.

Split length vs splitting score

A simple linear regression model was constructed to determine if the splitting scores method currently being used is a viable predictor for the lengths of board splits. The splitting scores across all trees were compared to the split lengths on each board from the respective trees and equation 11 was obtained.

$$SL = 732.67SS + 54.9 \qquad \textit{Equation 11}$$

Where

SL = split length (in mm)

SS = Diameter corrected splitting score (as calculated by equation 6)

The R^2 value of 0.2157 proved that the current means of scoring trees for splits is relatively inaccurate for predicting the length of splits in the sawn boards.

After analyzing all relevant data, different trends began to emerge for the various properties as seen in chapter 4. These trends provided insight into the effectiveness of the chosen methods of assessment for each property, and whether or not they could be used as viable predictors for the problematic properties. A bigger emphasis was placed on splitting and brittle heart as the primary concerns of this study over the other properties as they had the highest impact on the sawn board quality.

Strain was measured using the newly developed paddle core method. In theory, this method has the potential to identify stems with high growth stress; however, the method needs to be developed further to increase the accuracy. Trees which contained no reaction wood should have a strain graph which resembles figure 2 – 1, with maximum stress at the pith and bark, and a zero-point in between as the stress changes from a compressive force to a tensile force (Kamarudin, 2014). This was not the case for the strain measured in this experiment. Figure 4 – 11 shows the general pith to bark trend exhibited by growth stress. However the negative strain values indicates that the entire stem contained tensile growth stresses. Similarly, the mean for all groups in figure 4 – 12 suggests the presence of only tensile growth stresses. This implies that there was a possible error in the tools used to collect the samples. The discrepancy between the data from the two marking tools, with tool A providing only negative measurements and tool B positive measurements, also indicated a high probability of the tools being the cause of the irregularities in the data, However, the method seems to have potential for growth strain measurement, but the marking tool needs improvement.

5. Conclusion and recommendations

The ultimate objective of this project was to non-destructively measure, on standing Eucalyptus trees that differ in genotype and age, the properties such as strain, density, MC and ToF related to board splitting, brittle heart, shrinkage, and cell collapse,, and to assess the suitability of using these non-destructive methods as a predictive tool for identifying plus trees. To achieve this, it was therefore necessary to first describe the variation in wood properties within and between such trees

Property analysis showed that **split length** of the boards increased with age. The young groups, YI and YU, were significantly different to the mature groups, MI and MU, as well as the OLD and ST group – with the ST group having the highest mean split length. There was no statistical difference for genetic groups, however, the improved groups appeared to have slightly higher split length means. The mean split length decreased with **board** positions from the pith to bark, and with height. Board positions zero and one at the pith were both significantly different to all other positions with positions two and three near the bark being significantly lower but having no difference between the two positions.

Brittle heart in trees also increased with age and decreased with radial position and height. Brittle heart only started developing in the tree stems after 6 years of age. Brittle heart mainly progresses in board position zero over time, with it having substantial more brittle heart over time compared to board positions one, two and three.

Lengthwise **cell collapse** in boards, due to drying, proved to be concentrated in the centre of the tree, i.e. having the most influence on boards found in positions zero and one, with little to no collapse manifesting in positions two and three. Furthermore, cell collapse increased significantly with height for groups YU, MU and OLD in the centre region of the tree alone (in positions zero and one).

Width shrinkage of boards was low for the mature groups MI and MU, with shrinkage increasing for the young and older groups YI, YU, OLD and ST. The only significant difference for height was in group YI where log A exhibited significantly more shrinkage than log B. Width shrinkage also increased significantly from pith to bark, with all board positions being

significantly different from each other. Thickness shrinkage on the other hand decreased from pith to bark with board position zero being significantly different to positions two and three, and position one being significantly different to position three alone.

The **pith-to-bark density** profile obtained from the samples sticks showed a combination of decreasing and increasing trends from pith to bark (V-shaped). Density decreased from position zero to one and then increased from position one to two to three in all groups except MU where the minimum density was observed at position two. Furthermore, all the mature and older groups had a significant difference between the mean densities for the position with the minimum observed density and maximum observed density (namely between positions one and three).

Strain measured on the paddle cores which were marked with tool A showed an increase with board position for groups YI, OLD and ST, with no difference between ages per board position. Strain measured on the paddle cores which were marked with tool B showed a significant difference between genetic groups with the improved groups YI and MI having significantly less strain than the unimproved groups YU and MU respectively. The vast difference in results which occurred between marking tools A and B were unexpected as the general strain trend from pith-to-bark is expected to exhibit tensile and compressive forces, However, with the general pith-to-back trend displayed by tool A, this method proves to have potential with further refinement.

For pith-to-bark **MC**, all groups had significantly higher MC in log A at the base of the tree than log B further up the stem , with the exception of the unimproved groups YU and MU, which had no difference between the two logs. MC also had an unexplainable trend from pith to bark when MC increased from pith to bark for log A, but decreased for log B.

ToF measurements on the outer tree stem decreased significantly with age and with improved genetic material as the improved groups YI and MI had significantly smaller flight times than that of the unimproved groups YU and MU. Groups OLD and ST had the lowest mean flight time of all groups. The flight times between transducers indicates higher related stiffness in the improved groups which is positively related to strength as expected.

Cup showed various radial trends for the different groups. YI, YU and OLD had decreasing cup with increased position from the pith, whilst MU displayed the opposite trend. Groups MI and ST had no significant difference between any of the board positions. Cupping also increased significantly with height as log A had a significantly higher mean than log B.

For cupping, groups YI, YU and ST had no radial significant difference, whilst groups MI and OLD had increasing trends from pith to bark.

Lastly, **bow** increased significantly from pith to bark with each board position being significantly different to the rest.

For the correlations between properties, split length had positive correlations with split width (r = 0.60), log splitting score (r = 0.5), brittle heart (r = 0.38) and ToF (r = -0.33). Similarly, split width also has positive correlations with brittle heart (r = 0.46) and splitting score (r = 0.38), and negative correlations with the ToF (r = - 0.33). Collapse did not show moderate correlations with any of the other properties – only significant but weak correlations with ToF and log splitting score. Width shrinkage was correlated to density (r = 0.37) and brittle heart (r = - 0.31). Surprisingly, the strongest correlations were with moisture content (r = 0.38) and the ToF (r = 0.34).

A few predictive models were developed using the properties of MC, density, ToF and strain at the board level to predict the occurrence of splitting, brittle heart, cell collapse and shrinkage. Only one model had a moderate to good marginal r^2 = 0.772 (Model 1), which predicted split length in boards from the **young trees** of both groups YI and YU only, thus reiterating the title and aim of this research to predict using young trees. This model accepted moisture content, strain and ToF measurements as independent variables with the influence, as determined with sensitivity analyses, of each being 37%, 11% and 30% respectively. As mentioned previously, MC was measured destructively in discs, but this could be measured using the paddle cores as well for a less destructive means of obtaining the needed data. Unfortunately, no other model performed nearly as well with the next best model for predicting collapse having a mere marginal r^2 = 0.332.

With the use of sampling methods of limited-to-no destruction such as the paddle core method used in this study, properties which would otherwise be unmeasurable in standing trees can now be assessed. This includes density, moisture content and strain along with properties not used in this study (such as cellulose, lignin and extractive contents too). This increases the variety of property data for analysis to determine whether the given standing trees are of good or poor quality. Such improvements are vital to the success of any tree breeding programme where it is impossible to sacrifice the stem for destructive evaluation.

Furthermore, the tree splitting score method by Conradie (1980) which utilizes scores from a minimum of four log faces per tree was compared solely to the length of board splits, where a poor coefficient of determination was found between the two with r^2=0.216 indicating that splitting score is not a good indicator of sawn board split length.

Despite the discrepancies which arose from the strain measurements, the model built to determine the severity of split length in young trees had a relatively high coefficient of determination with marginal r^2=0.772. Therefore, it is satisfactory to predict split length for young trees when MC, density, ToF and strain are assessed.

Given the outcomes of this study, a recommendation for future research into this topic is to start with a pilot study, to help eliminate any unforeseeable problems with regards to data collection. A more accurate method for measuring strain from the paddle core is also advisable as strain measurements are very precise and measured in microns, Furthermore, it would be advisable to do single specie comparisons for any experiments related to genetic improvements or modifications as multi-specie comparisons introduce an additional variable in an already complex research field.

References

1. Ananías RA, Sepúlveda-Villarroel V, Pérez-Peña N, Leandro-Zuñiga L, Salvo-Sepúlveda L, 767 Salinas-Lira C, Cloutier A, Elustondo DM. 2014. Collapse of *Eucalyptus nitens* wood after drying depending on the radial location within the stem. Drying Technology 32(14): 1699-1705.
2. Bailleres, H.; Chanson, B.; Loup, C.; Fournier, M. And Gérard, J., 1992. Constraints of maturation according to height and age in young *Eucalyptus* plantation. Proceedings IUFRO V, Nancy, France, 23-28 August 1992.
3. Bariska M (1992) Collapse phenomena in *eucalypts*, Wood Science and Technology, 26:165-179
4. Barros E, Verryn S and Hettasch M (2002) Identification of PCR-based markers linked to wood splitting in *Eucalyptus* grandis. Annals of Forest Science, 59(5-6) pp.675-678
5. Biechele, T., Nutto, L. & Becker, G. (2009). Growth strain in *Eucalyptus nitens* at different stages of development. Silva Fennica 43(4): 669–679.
6. BHA T, K.M.; BHA T, K. V. and DHAMODARAN, T.K., 1990. Wood density and fibre length of ***Eucalyptus grandis*** grown in Kerala, India. *Wood and Fibre Science,* Vol. 22, No 1, pp. 54 - 61Biechele, T., Nutto, L. & Becker, G. 2009. Growth strain in *Eucalyptus* nitens at different stages of development. Silva Fennica 43(4): 669–679.
7. Chafe S.C., (1985) The distribution and interrelationship of collapse, volumetric shrinkage, moisture content and density in trees of *Eucalyptus regnans* F.Muell. Wood Science and Technology 19:329-345
8. Chafe, C.S., (1986) Radial variation in collapse, volumetric shrinkage, moisture content and density in *Eucalyptus* regnans F. Muell. Wood Science and Technology 20:253-262
9. Chauhan, S.S. and Walker, J. (2004) Relationships between longitudinal growth strain and some wood properties in *Eucalyptus nites*, Australian Forestry 67(4):254-260
10. Christoforo, A.L., de Almeida, T.H., de Almeida, D.H., dos Santos, J.C., Panzera, T.H. and Lahr, F.A.R., (2016) Shrinkage for Some Wood Species Estimated by Density, International Journal of Materials Engineering 6(2):23-27
11. Clark, A. and Daniels, R.F., (2000), Estimating moisture content of tree-length roundwood. Pulping/Process and Product Quality Conference, Sheraton Boston.
12. Clarke, S. A. 1927: The seasoning of Western Australia hardwoods. Forest. Dept. West. Austr. Bull. 40

13. Conradie WE (1980) Utilization of South African grown *Eucalyptus* grandis (W. Hill ex Maiden) as veneer logs. Part 1. Control of end splitting in veneer logs. CSIR Special Report, Hout 206. Council for Scientific and Industrial Research, Pretoria.

14. Dadswell, H.E. and Langlands, I. (1938), Brittle heart and its relation to compression failures, Empire Forestry Journal 17(1):58-65

15. Desch, H.E. and Dinwoodie, J.M. (1981) *Timber: It's structure, properties and utilization*. 6th Edition. The MacMillan Press Ltd.+

16. Downs, G., Meder, R., Ebdon, N., Bond, H., Evans, R., Joyce, K. and Southerton, S., (2010), Radial variation in cellulose content and kraft pulp yield in *Eucalyptus* nitens Using near-infrared (spectral analysis of air-dry wood surfaces. Journal of Near Infrared Spectroscopy 18(2):147-155

17. Downes, G., Harwood, C., Weidemann, J., Ebdon, N., Bond, H. and Meder, R., (2012) Radial variation in craft pulp yield and cellulose content in *Eucalyptus* globulus wood across three contrasting sites predicted by near infrared spectroscopy. Canadian Journal of Forest Research 42(8):1577-1586

18. Ekevad, M., Lundgren, N. and Flodin, J. (2011) Drying shrinkage of sawn timber of Norway spruce (*Piceaabies*): Industrial measurements and finite element simulations, Wood Material Science and Engineering, 6:1-2, 41-48

19. Godsmark R (2017) The South African Forestry and Forest Products Industry, Forestry South Africa

20. Githiomi JK, Kariuki JG (2010) Wood basic density of *Eucalyptus* grandis from plantations in central rift valley, Kenya: variation with age, height level and between sapwood and heartwood. J Trop For Sci 22:281–28

21. Gonya, N.A.S., (2020) An investigation into shrinkage and collapse behavior of *Eucalyptus* grandis and *Eucalyptus grandis X urophylla* wood. University of Stellenbosch.

22. Grabianowski M, Manley B, Walker JCF (2006) Acoustic measurements on standing trees, logs and green lumber. Wood Science and Technology 40:205-21

23. Hardie A.D.K. (1974) Defects in the wood of fast-grown *Eucalyptus* grandis in Zambia. The Forestry Association Review53(4):310-317

24. Hein, P.R.G., Siva, J.R.M., Brancheriau, L. 2013. Correlations among microfibril angle, density, modulus of elasticity, modulus of rapture and shrinkage in 6-year-old *Eucalyptus* urophylla x E. grandis. Maderas. Ciência Y Technologia, 15(1): 171-182.

25. Hein, P.R.G., Brancheriau L., Radial variation of microfibril angle and wood density and their relationship in 14-year old *Eucalyptus* urophylla S.T. Blake Wood.

26. Ivkovic M., Gapare W.J., Abarquez A., Ilic J., Powell M.B. and Wu H.X. (2009) Prediction of wood stiffness, strength, and shrinkage in juvenile wood at radiata pine. Wood Science and Technology 43:237-257

27. Isik, F. and Li, B. (2003) Rapid assessment of wood density of living trees using the Resistograph for selection in tree improvement programs. Canadian Journal of Forest Research. 33:2426-2435

28. Johnstone, D.M., Ades, P.K., Moore, G.M. and Smith, I.W., (2007) Predicting Wood Decay in *Eucalyptus* using an Expert System and the IML-Resistograph Drill. Arboriculture and Urban Forestry 33(2):76-82

29. Kamarudin N (2014) A new technology for measuring growth stress in *Eucalyptus*.
30. Kord B, Kialashaki A, Kord B. 2010. The within-tree variation in wood density and shrinkage, 825 and their relationship in Populus euramericana. Turkish Journal of Agriculture and 826 Forestry 34: 121–126.
31. Kübler, H. 1959. Die Spannungen in Faserrichtung. Holz alsRoh- und Werkstoff 17(2): 44–54.
32. Leonardon M, Altaner CM, Vihermaa L and Jarvis M (2010) Wood shrinkage: influence of anatomy, cell wall architecture, chemical composition and cambial age. European Journal of Wood Products 68:87-94
33. Malan F.S. and Gerischer GFR (1987) Wood property differences in South African Grown *Eucalyptus* grandis trees of different growth stress intensity. Holzforschung 41(6):331-335
34. Malan F.S. (1995) *Eucalyptus* improvement for lumber production. Division of Forest Science and Technology, CSIR, South Africa
35. Malan F.S., (2008) Clonal differences in log end splitting in *Eucalyptus grandis* in relation to age, parent performance, growth rate and wood density in two even-aged trials in Mpumalanga, South Africa, Southern Forests: A Journal of Forest Science, 70:1, 37-43, DOI:10.2989/SOUTH.FOR.2008.70.1.7.517
36. Mannes D et al (2007) Neutron imaging verses X-ray densitometry as a method to measure tree ring wood density. Trees 21:605-612

37. McKenzie, H.M., Shelbourne, C.J.A., Kimberly, M.O., McKinley, R.B. and Britton, R.A.J., (2002) Processing young plantation-grown *Eucalyptus nitens* for solid-wood products. 2: Predicting product quality from increment core, disc and 1-m billet properties. New Zealand Journal of Forest Science 33(1):79-113
38. Medhurst, J., Ottenschlaeger, M., Wood, M., Harwood, C., Beadle, C. and Valencia, J.C., (2011) Stem eccentricity, crown dry mass distribution, and longitudinal growth strain of) plantation-grown *Eucalyptus nitens* after thinning, Canadian Journal of Forest Research 41(11):2209-2218
39. Okuyama T, Doldan J, Yamamoto H and Ona T (2003) Heart splitting at crosscutting of eucalypt logs. Journal of Wood Science 50:1-6
40. Orwa, C., Jamnadass, R.H., Kindt, R., Mutua, A. and Simons, A. (2009) Agroforestree database: a tree species reference and selection guide version 4.0. World Agroforestry Centre ICRAF, Nairobi, KE
41. Priadi, I.T., (2001). A study of pre-treatment in the drying of regrowth *Eucalyptus obliqua L'herit.* University of Tasmania. MEngSc.
42. Priest, D.T, Knuffel, W.E. and Malan, F.S, 1982, End-splitting in E.grandis sawlogs and sawn timber.CSIR Special Report, Hout, 223.
43. Purnell, R.C., (1988) Variation in Wood Properties of Eucalyyptus nitens in a Provenance Trial on the Eastern Transvaal Highveld in South Africa, South African Forestry Journal, 144(1):10-22
44. Raymond CA, Kube PD, Pinkard L, Savage L and Bradley AD (2003) Evaluation of non-destructive methods of measuring growth stress in *Eucalyptus* globulus: relationships between strain, wood properties, and stress. Forest Ecology and Management 190:187-200
45. Schimleck, L.R., Evans, R. and Ilic, J., (2001) Estimation of *Eucalyptus* delegatensis wood properties by near infrared spectroscopy. Canadian Journal of Forest Research 31:1671-1675
46. Sepulveda P (2001) Measurement of spiral grain with computed tomography. Journal of Wood Science 47:289-293
47. Shi-jun WU, Jian-min XU, Guang-you LI, Vuokko RISTO, Zhao-hau LU, Bao-qi LI and Wei WANG (2010) Use of the pilodyn for assessing wood properties in standing trees of *Eucalyptus* clones, Journal of Forestry Research 21(1):68-72
48. "Silviscan™ Rapid Wood Analysis - Csiropedia". CSIROpedia. [Online]. Available: https://csiropedia.csiro.au/silviscan-rapid-wood-analysis/ [2017, March 27].

49. Smith DM (1954) Maximum moisture content method for determining the specific gravity of small wood samples. Report 2014, United States Department of Agriculture
50. Thomas, E.V., (1994) A primer on multivariate calibration. Analytical Chemistry 66(15): A795-A804
51. Tsoumis, G. (1991), Science and Technology of Wood. Structure, Properties, Utilization. House Kessel.
52. Valencia, J., Harwood, C., Washusen, R., Morrow, A., Wood, M. and Volker, P., (2011) Longitudinal growth strain as a log and wood quality predictor for plantaion-grown *Eucalyptus* nitens sawlogs. Wood Science and Technology 45:15-34
53. Vermaas, H.F. (2000) Primary processing of *eucalyptus* and factors affecting it. The Southern African Forestry Journal, 187(1):37-44
54. Verryn, S.D. and Turner, P. (2000) The prediction and selection of solid *E.grandis* solid wood: Phase one. Division of Water, Environment and Forestry Technology, CSIR, Pretoria
55. Wahyudi, I., Okuyama,T., Hadi, Y.S., Yamamoto, H., Yoshida, M. and Watanabe, H. (1999) Growth stresses and strains in Acacia mangium, Forest Products Journal 49(2):77-81
56. Wentzel-Vietheer, M., Washusen, R., Downes, G.M., Harwood, C., Ebdon, N., Ozarska, B. and Baker, T., (2013), Prediction of non-recoverable collapse in *Eucalyptus* globulus from near infrared scanning of radial wood samples, European Journal of Wood and Wood Products, 71:755-768
57. Wessels, C.B., Malan, F.S. and Rypstra T., (2011), A review of measurement methods used on standing trees for the prediction of some mechanical properties of timber. European Journal of Forest Research, 130:881-893.
58. Wilkins AP, Horne R. 1991. Wood-density variation of young 893 plantation-grown *Eucalyptus,* 894 *grandis* in response to silvicultural treatments. Forest Ecology and Management 40: 39-50
59. Wu, Y., Hayashi, K., Liu, Y., Cai, Y., Sugimori, M. and Luo, J. 2005. Collapse-type shrinkage characteristics in plantation-grown *Eucalyptus*: I. Correlation of basic density and some structural indices with shrinkage and collapse properties. Journal of Forestry Research, 16(2): 83-88.

60. Yamashita, K., Hirakawa, Y., Nakatami, H. and Ikeda, M., (2009) Tangential and radial shrinkage variation within trees in sugi (Cryptomeria japonica) cultivars, Journal of Wood Science 55:161-168
61. Yang J.L., Edward, F. (1995) Investigation for brittleheart in two *Eucalyptus* Regnans logs, Forest Products Journal; Madison Vol.45 Issue 11.12
62. Yang J.L. (2001), Bending strength properties of regrowth Eucalypt brittleheart. Holzforschung 55:183-184
63. Yang, J.L. and Waugh, G. (2001), Growth stress, its measurements and effects, Australian Forestry 64(2): 127-135
64. Zanuncio, A.J.V., Carvalho, A.G., da Silva, L.F., Lima, J.T., Trugilho, P.F., da Silva, J.R.M. 2015. Predicting moisture content from basic density and *Eucalyptus* and *Corymbia* logs. *Ciencia y tecnología*, 17(2): 335 – 344.

Appendix A

Appendix A - 1: ANOVA information for graph in Figure 4 – 6.

Position	Group	Log	lsmean	SE	df	lower.CL	upper.CL	.group
zero	YI	A	0.222	2.92	887	-5.518	5.96	abc
zero	YI	B	2.222	2.92	887	-3.518	7.96	abcde
zero	YU	A	5.000	2.77	887	-0.446	10.45	abcdef
zero	YU	B	21.333	2.92	887	15.593	27.07	i
zero	MI	A	7.500	2.77	887	2.054	12.95	bcdefg
zero	MI	B	10.500	2.77	887	5.054	15.95	fg
zero	MU	A	8.333	2.92	887	2.593	14.07	cdefg
zero	MU	B	19.000	2.77	887	13.554	24.45	hi
zero	OLD	A	9.545	2.65	887	4.353	14.74	efg
zero	OLD	B	29.545	2.65	887	24.353	34.74	j
zero	ST	A	0.588	2.13	887	-3.588	4.76	a
zero	ST	B	0.263	2.01	887	-3.688	4.21	a
one	YI	A	1.667	2.07	887	-2.392	5.73	abc
one	YI	B	0.588	2.13	887	-3.588	4.76	a
one	YU	A	6.850	1.96	887	2.999	10.70	cdef
one	YU	B	4.500	2.07	887	0.441	8.56	abcdef
one	MI	A	2.250	1.96	887	-1.601	6.10	abc
one	MI	B	4.750	1.96	887	0.899	8.60	abcdef
one	MU	A	8.056	2.07	887	3.997	12.11	defg
one	MU	B	13.600	1.96	887	9.749	17.45	gh
one	OLD	A	2.211	2.01	887	-1.740	6.16	abc
one	OLD	B	18.750	2.19	887	14.445	23.06	hi
one	ST	A	1.774	1.58	887	-1.319	4.87	ab
one	ST	B	0.345	1.63	887	-2.853	3.54	a
two	YI	A	0.000	1.66	887	-3.254	3.25	a
two	YI	B	0.000	1.91	887	-3.758	3.76	a
two	YU	A	0.435	1.83	887	-3.156	4.03	a
two	YU	B	0.385	2.43	887	-4.392	5.16	ab
two	MI	A	3.000	1.96	887	-0.851	6.85	abcd
two	MI	B	0.167	1.60	887	-2.977	3.31	a
two	MU	A	0.238	1.91	887	-3.520	4.00	a
two	MU	B	1.074	1.69	887	-2.240	4.39	a
two	OLD	A	0.217	1.83	887	-3.373	3.81	a
two	OLD	B	4.118	2.13	887	-0.059	8.29	abcdef
two	ST	A	0.000	1.42	887	-2.794	2.79	a
two	ST	B	0.694	1.46	887	-2.176	3.56	a
three	YI	A	0.000	3.10	887	-6.088	6.09	abc
three	YI	B	0.000	4.39	887	-8.610	8.61	abcde
three	YU	A	0.000	3.10	887	-6.088	6.09	abc
three	YU	B	0.000	6.20	887	-12.177	12.18	abcdef
three	MI	A	1.130	1.29	887	-1.409	3.67	a
three	MI	B	0.208	1.79	887	-3.307	3.72	a
three	MU	A	0.000	1.72	887	-3.377	3.38	a
three	MU	B	0.250	3.10	887	-5.838	6.34	abc

three	OLD	A	0.227	1.32	887	-2.369	2.82	a
three	OLD	B	0.000	1.72	887	-3.377	3.38	a
three	ST	A	0.909	1.53	887	-2.089	3.91	a
three	ST	B	0.172	1.63	887	-3.025	3.37	a

Appendix B

Figure B - 1: Log 63A - 3 days after felling vs 5 days after felling.

Appendix C

Related predictive models produced by other studies.

Model C – 1: Longitudinal growth strain as modeled by Valencia et al. (2011)

Y = mean + dbhob X thinning X aspect + tree + residual *Equation C - 1*

Where

Y = longitudinal growth strain

mean = overall mean

dbhob = over bark diameter

thinning = thinning treatment

aspect = measurement aspect

With tree and residual as random effects. The effects of strain on the processing traits for the Valencia study is listed below in Table C - 1

Table C - 1: Performance traits with regards to longitudinal growth strain as predicted by Valencia et al. (2011) for the Model C - 1 as produced by Valencia et al.

Processing trait	Factors included[a]	r^2 (%) without LGS	Extra gain in r^2 due to LGS	Relationship[b]
SPLITINDEX-BUTT	DBHOB LOG	34.2	14.6	Positive
SPLITINDEX-TOP	DBHOB LOG	18.2	17.8	Positive
SPLITINDEX-SUM	DBHOB LOG	25.0	19.5	Positive
Flitch distortion	LOG	4.2	0.3	Positive
Slab distortion	LOG	14	0	
Slab distortion	LOG SPLITINDEX-SUM	18	0	
Bow-green	SAWMETH	42.9	3	Positive
Bow-green	SAWMETH SPLITINDEX-SUM	47.0	1	Positive
Bow-dry	SAWMETH	39	2	Positive
Bow-dry	SAWMETH SPLITINDEX-SUM	41	1	Positive
Spring-green	SAWMETH DBHOB	2.8	1.2	Positive
Spring-dry	SPLITINDEX-SUM	0.7	0.5	Positive
Mean shrinkage width	SAWMETHOD	35.2	0.2	Positive
Mean shrinkage width	SAWMETHOD SPLITINDEX-SUM	36.3	0	
Board end split extent-dry	SAWMETH DBHOB LOG	5.4	2.1	Positive
Loss from end docking-green	SAWMETH DBHOB LOG	5.4	2.1	Positive
Loss from end docking-green	SAWMETH DBHOB LOG SPLITINDEX-SUM	10.3	0.3	Positive
Total recovery	SAWMETH DBHOB	11	1.3	Negative
Total recovery	SAWMETH DBHOB SPLITINDEX-SUM	12.8	0.4	Negative

[a] Significant ($P < 0.05$) in the mixed models analysis

[b] Relationship between LGS and processing trait

Model C – 2: Tangential shrinkage as modeled by Wentzel-Vietheer et al. (2013)

$$Y = -26.109 + (0.679)X1 + (0.382)X2 \qquad \textit{Equation C - 2}$$

where:

Y is the predicted tangential shrinkage to 12 % MC

X1 is the NIR-predicted cellulose content (%); and

X2 is the NIR-predicted MOE (GPa).